
Models for Energy Performance Analysis

Financed by The Danish Electricity Saving Trust

Peder Bacher
Anders Thavlov
Henrik Madsen

Informatics and Mathematical Modelling
Technical University of Denmark
DK-2800 Kongens Lyngby

January 5, 2010

IMM-Technical Report-2010-02



Contents

1	Introduction	5
1.1	Background	5
1.1.1	FlexHouse	5
1.2	Outline	6
2	Data preprocessing	7
2.1	Visual inspection	7
2.1.1	Interpolation of temperatures	9
2.1.2	Heater values	11
2.2	Principal component analysis	11
3	Models for the heat dynamics of a building	14
3.1	Heat dynamics	14
3.1.1	Heat Capacity	14
3.1.2	Heat Transfer	15
3.2	Modelling Approach	19
3.3	Grey-box model	20
3.3.1	Stochastic linear state space model	20
3.3.2	Measurement equation	23
3.4	Link to regression models	23
4	Parameter estimation	25
4.1	Stochastic linear state space model in discrete time	25
4.2	Maximum Likelihood Estimator	27
4.3	CTSM - Continuous Time Stochastic Modeling	29
4.3.1	Modelling in CTSM	29
4.4	Time constants	30
4.5	Tests for model expansion	30
4.5.1	Likelihood ratio tests	30
4.5.2	Hypothesis chains	31

5	Linear models	32
5.1	Selected models	32
5.1.1	Linear A	33
5.1.2	Linear B	33
5.1.3	Linear C	34
5.1.4	Linear D	35
5.1.5	Linear E	36
5.2	Model selection	37
5.2.1	From Linear A to Linear B	37
5.2.2	From Linear B to Linear C	38
5.2.3	From Linear C to Linear D	39
5.2.4	From Linear D to Linear E	39
5.3	Tests of expansions and submodels of Linear E	39
6	Analysis of the one-step prediction error	41
6.1	Mean and variance of the one-step prediction error distribution	41
6.2	Linear A	42
6.3	Linear B	42
6.4	Linear C	42
6.5	Linear D	43
6.6	Linear E	43
7	Results	49
7.1	Rough physical values	49
7.1.1	Heat capacities	49
7.1.2	Window area	50
7.2	Estimated physical parameters and time constants	51
7.2.1	Heat capacities	51
7.2.2	R-values and UA-values	52
7.2.3	Window area	52
7.2.4	Time constants	52
8	Further work	54
8.1	Modelling with the present data	54
8.2	Carrying out further experiments	54
9	Conclusion	56
A	Input data to CTSM	57

Acknowledgement

We would like to thank Henrik Bindner and the people at VEA Risø DTU ¹ which apart from providing the experimental facilities, has helped all the way through the work. The work would not have been possible without the support from the Danish Electricity Saving Trust (Elsparefonden²) especially Poul Erik Pedersen, and the comments and advices from the project group especially Søren Østergaard Jensen, Bjarne W. Olesen, Carsten Rode, Henrik Aalborg Nielsen, and Kim B. Wittchen.

¹http://www.risoe.dk/About_risoe/research_departments/VEA.aspx

²<http://www.savingtrust.dk>

Chapter 1

Introduction

1.1 Background

Approximately one third of the primary energy production in Denmark is used for heating the air in buildings and therefore efforts to improve energy performance of the building mass will have large impact on the total energy consumption. A model of the heat dynamics of a building can be used to obtain knowledge of the energy performance of the building. This can especially be used in the effort to decrease the energy consumption by increasing the awareness of the energy performance to the residents of the building.

In the present study models are developed of the heat dynamics in FlexHouse which is an experimental building located at Risø DTU. The aim of the study is to develop models of different complexity, which can estimate the physical quantities that influence the heat dynamics of the building, such as UA-values and time constants. The models use climate observations measured at the location and air temperature measurements from sensors inside the building. Furthermore the aim is to gain knowledge of which features of the models that can be used to inform about the effect of energy saving initiatives for the building.

Numerous approaches for modelling the heat dynamics of a building are found in the literature. They can be divided into deterministic methods and stochastic methods. [4] gives an overview of computer-aided building simulation tools presenting the approaches and applications. The present study uses methods developed by [7] and [1] where stochastic differential equations are applied.

1.1.1 FlexHouse

FlexHouse is an office building located at Risø DTU, the National Laboratory for Sustainable Energy. The energy supply to FlexHouse is purely electrical. The size of FlexHouse is approximately 125 m² divided between eight rooms and a toilet. The rooms have been numbered 0 to 7 to distinguish between them. A layout of FlexHouse can be seen in Figure 1.1 where also the room numbers are shown. Room 1–7 are arranged as small offices, each with a desk, office chair and a computer. The main room, room 0, has been furnished with

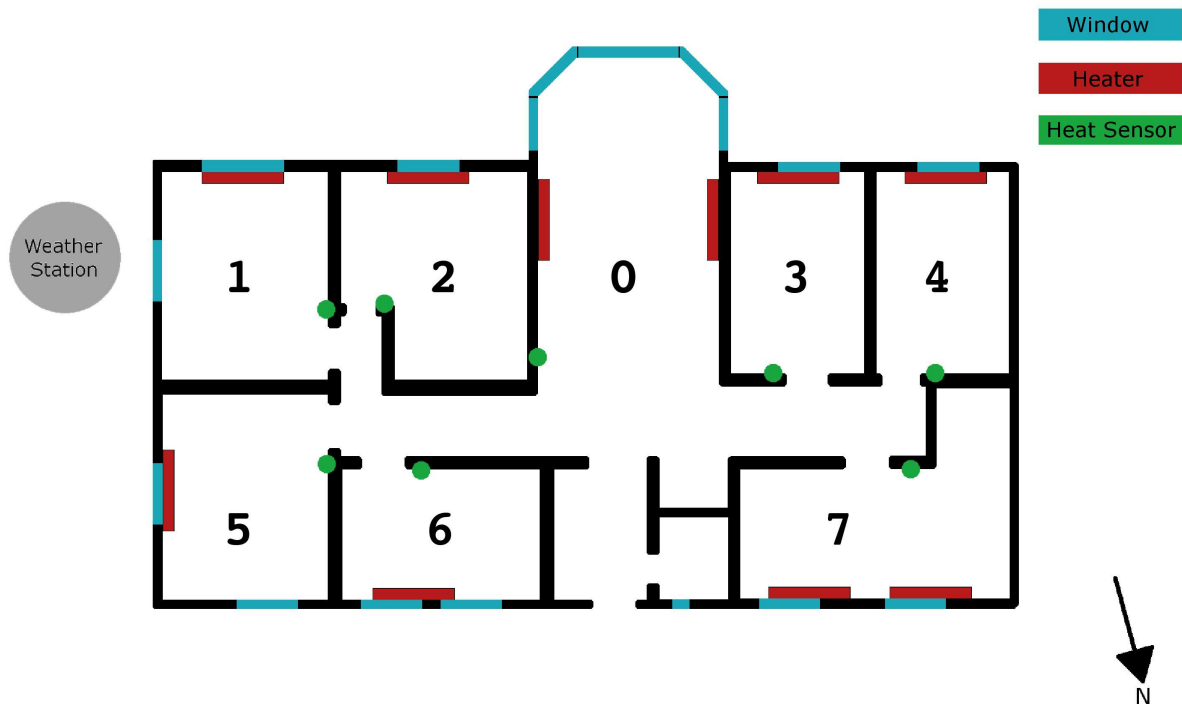


Figure 1.1: FlexHouse layout

tables and chairs to accommodate meetings. Moreover room 0 contains a small kitchen with a refrigerator and a coffee machine. The southern wall in the main room is dominated by a large window facade. From the main room access to a toilet is possible, where the water heater is placed. Electrical space heaters are mounted in room 1–6, whereas room 0 and 7 each has two heaters mounted. FlexHouse are build from light building materials. The building envelope consist of an outer layer of wood and an inner layer of plaster, with insolation material in the middle. The house is build upon poles and has an open space of air beneath. For more details of Flexhouse see [11].

1.2 Outline

The pre-processing of the data is described in Chapter 2. The physical heat transfer theory and modelling approach used in the study are outlined in Chapter 3, followed by a presentation of the statistical techniques used for parameter estimation in Chapter 4. The applied heat dynamics models and model selection are described in Chapter 5, and the results are presented and discussed in Chapter 7. Finally the conclusions are drawn in Chapter 9.

Chapter 2

Data preprocessing

The data used in the present study is described in [11]. This chapter describes an exploratory analysis and preprocessing of the data before it is applied to build the heat dynamics models. Plots of the entire dataset can be found in [11]. The data from experiment number three to six, that is the four successful experiments, are investigated. The preprocessed data used as input to the models is plotted in Appendix A.

The chapter starts by a visual inspection of the data to find outliers and unwanted effects. This lead to removal and correction of some parts of the data. Finally a single signal to represent the indoor temperature are found using principal component analysis.

2.1 Visual inspection

Visual inspection of the data reveal several unwanted effects in the dataset. The temperatures in each experiment are showed in Figure 2.1. It is seen that Experiment 5 differs from the other three experiments. This is because only two heaters were used in the experiment, and since only one indoor temperature signal will be used, the assumption of equal temperature in all areas of the house is not reasonable. Therefore Experiment 5 is removed from the dataset.

The plot also reveals that there seems to be a constant temperature difference among the rooms. Generally there is a difference around $5^{\circ}C$ from the lowest to highest temperature. Furthermore it seems that the temperature in the same room tend to be either in lower part or in the higher part, e.g. the temperatures in room 1, 5, 6, and 7 are mostly in the lower part, whereas the temperatures in the main room and room 2, 3, and 4 are mostly in the higher part. Either the real temperatures are different or each temperature sensor has a considerable bias. It is not found possible to conclude on this, but future experiments should cross validate the temperature sensors to check for bias.

The upper plot in Figure 2.2 is a plot of the temperatures in Experiment 6, and it can be seen that the signal from the temperature sensor in room 5 is abnormal in the morning hours the 27'th and 28'th of May, but normal in the morning of the 29'th. Considering the lower plot in Figure 2.2 of the global irradiance and the fact that room 5 is on the east

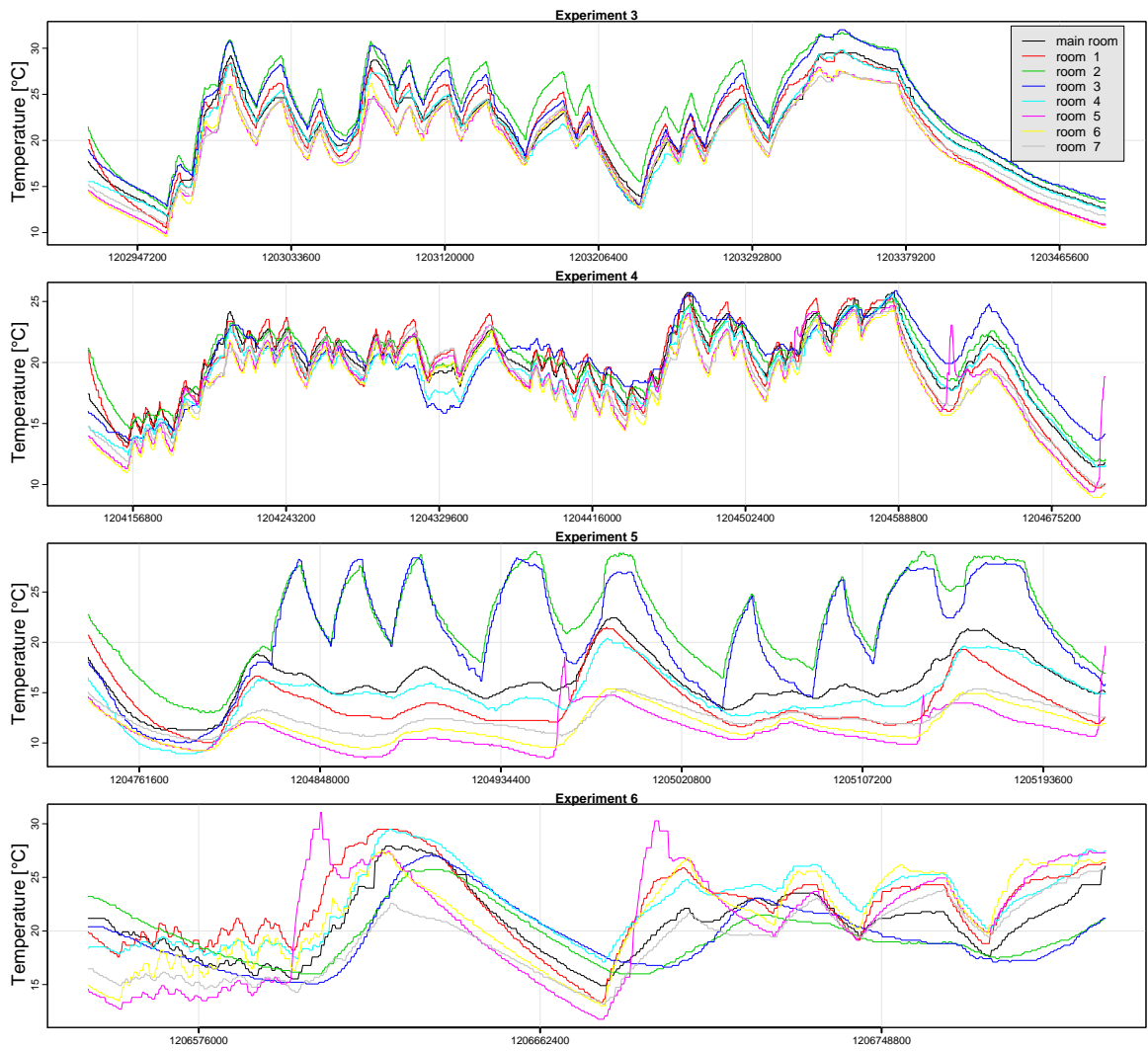


Figure 2.1: Plot of the temperature in each room.

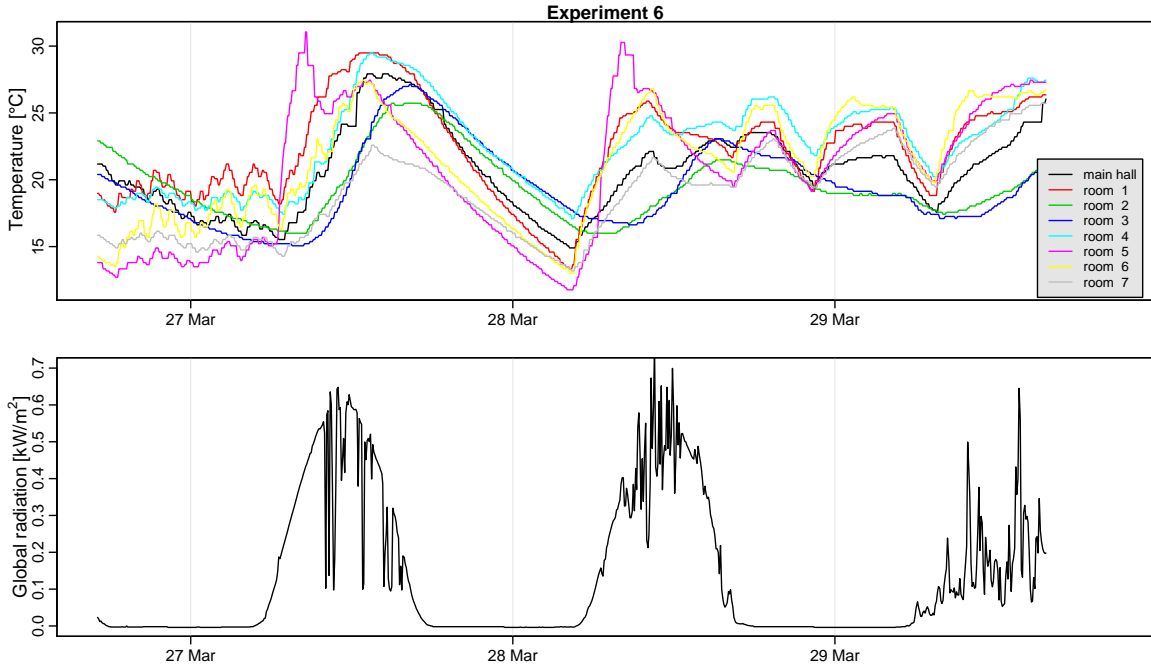


Figure 2.2: Upper plot is the temperature signal from each room in experiment 6. Lower plot is the corresponding global irradiance.

side of the building, it is clear that direct solar radiation strikes the sensor in mornings with a non-overcast sky. Parts of the signal is thus filled with outliers, and therefore the temperature signal from room 5 is removed from the dataset.

A plot of the global irradiance and the sine of the solar elevation in Figure 2.3 reveal that the time stamps of Experiment 3 are one hour ahead. This is simply corrected by adding one hour. This will not have a high effect in the present modelling, but generally synchronization of data should be checked. By comparing observed global irradiance with the sine of the solar elevation it is possible to reveal synchronization errors in weather data.

The experiments were designed to have a constant samplerate, but as seen in Figure 2.4 where the time between the sample points is plotted the random jitter is considerably high. This should be taken into consideration when parameters of the models are estimated.

2.1.1 Interpolation of temperatures

The temperature sensors installed in FlexHouse only send a value when the temperature has changed $\pm 0.5^\circ\text{C}$. This induce a constant value for most of the observed 5 minute temperature values, as seen by values from the main room plotted in Figure 2.5. Each temperature signal is smoothed by linear interpolation between points where the value has changed, as showed in the plot. An improvement of the interpolation could be accieved by applying higher order smoothing methods, and this should be considered in future applications.

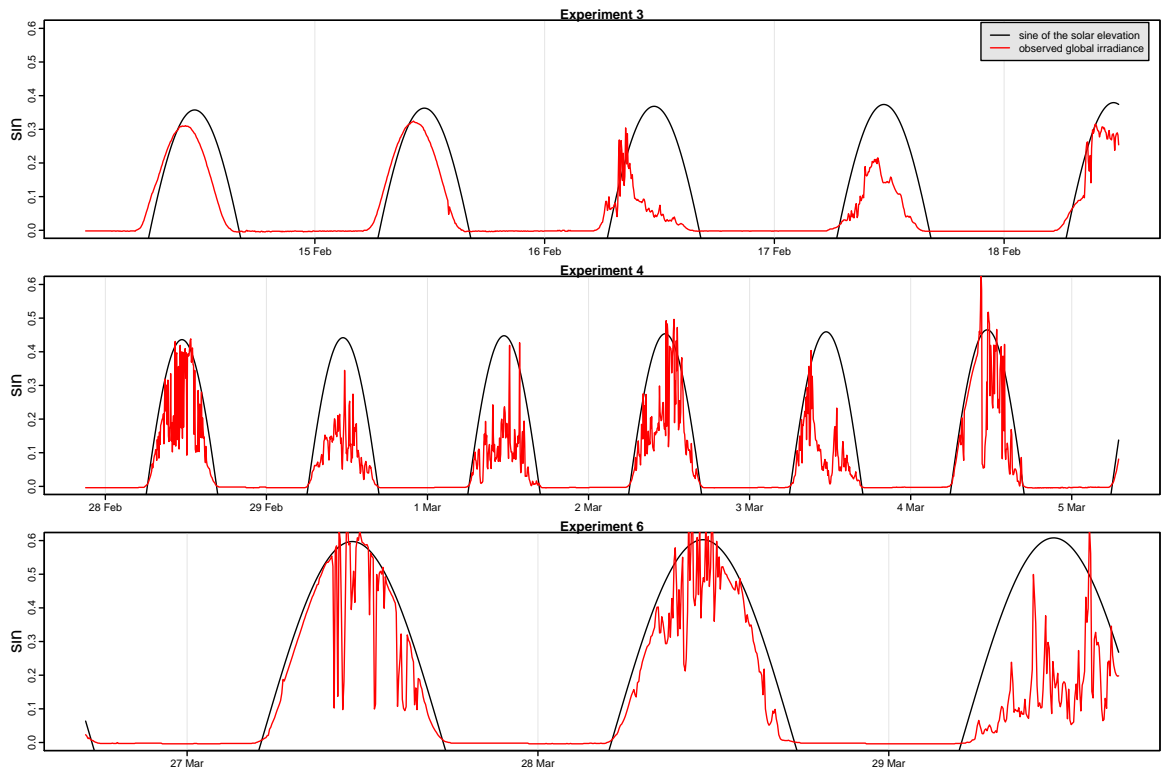


Figure 2.3: The global irradiance and sine of the solar elevation for experiment 3,4, and 6.

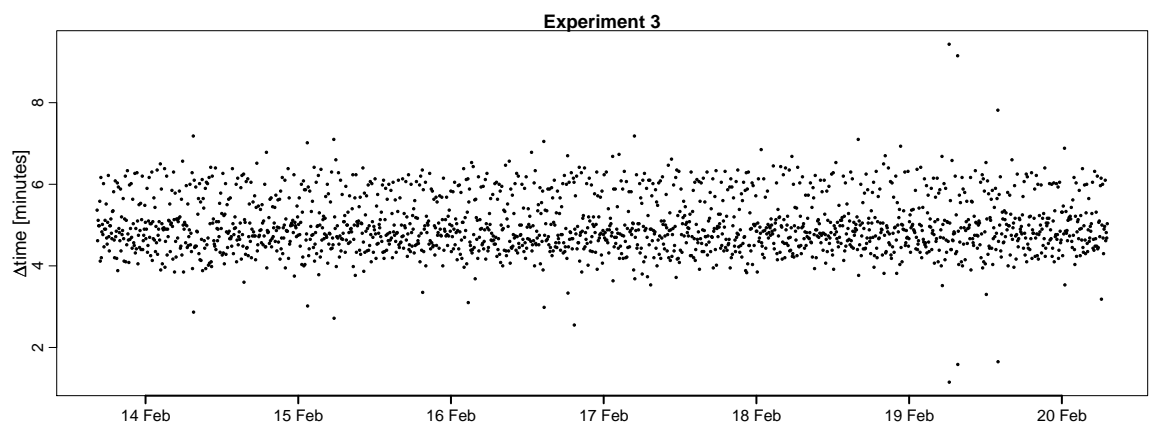


Figure 2.4: The times between each sample point in Experiment 3.

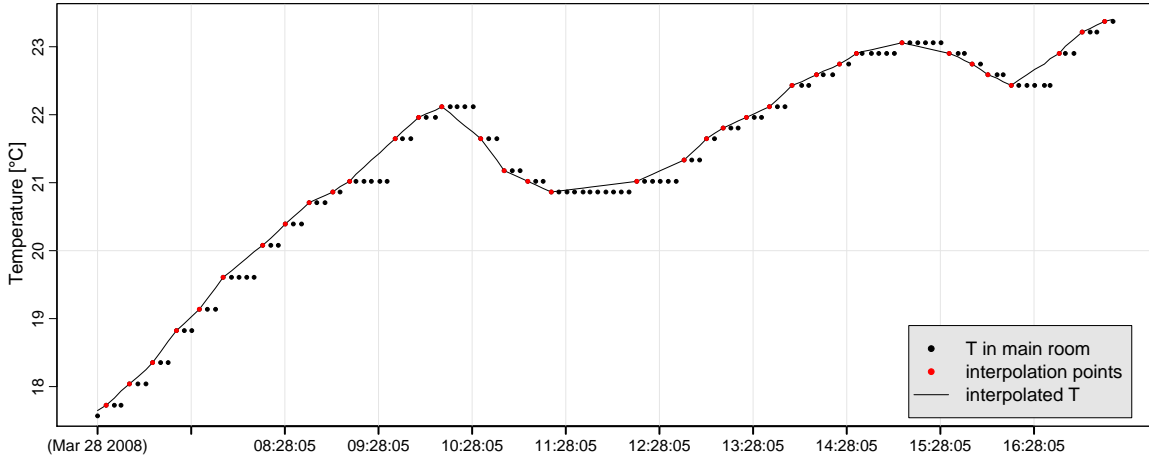


Figure 2.5: Interpolation of the temperature signals. The points are temperature observations from the main room in Experiment 6.

2.1.2 Heater values

The heat signal is the energy input to the house from the electrical heaters. At timepoints where the state, ie. either on or off, is shifted, the heat signal recorded during the experiments can be improved. The heat signal is modified as illustrated in Figure 2.6 where the real underlying heat input signal is showed together with the recorded and corrected values. During the experiments the state shifts at timepoints t_i , which is the timepoint where values of all signals are recorded. The recorded value at t_i represent the signal in the time interval

$$\left[t_i - \frac{t_i - t_{i-1}}{2} \quad t_i + \frac{t_{i+1} - t_i}{2} \right]. \quad (2.1)$$

The intervals from shifts in states are marked with grey in the plot. During an interval the real heat input is in each state approximately half of the time, and the recorded values of the the intervals are seen not to be correct. They are corrected to the integrated signal during the period, which is approximately 0.5. Finally the heat signal from all the heaters are summed to form Φ_h .

2.2 Principal component analysis

The applied heat dynamics models all use the approximation that the interior of the building is one room. The reason is that due to limitations in the control system of the electrical heaters in FlexHouse the PRBS signal was forced to be the same in all rooms. Therefore it is needed to transform the temperature signals from each room into one single representative signal. Principal component analysis (PCA) is used as suggested in [9].

Principal component analysis is a linear transformation of data. The data is transformed to an orthogonal coordinate system, such that the first axis is parallel to the

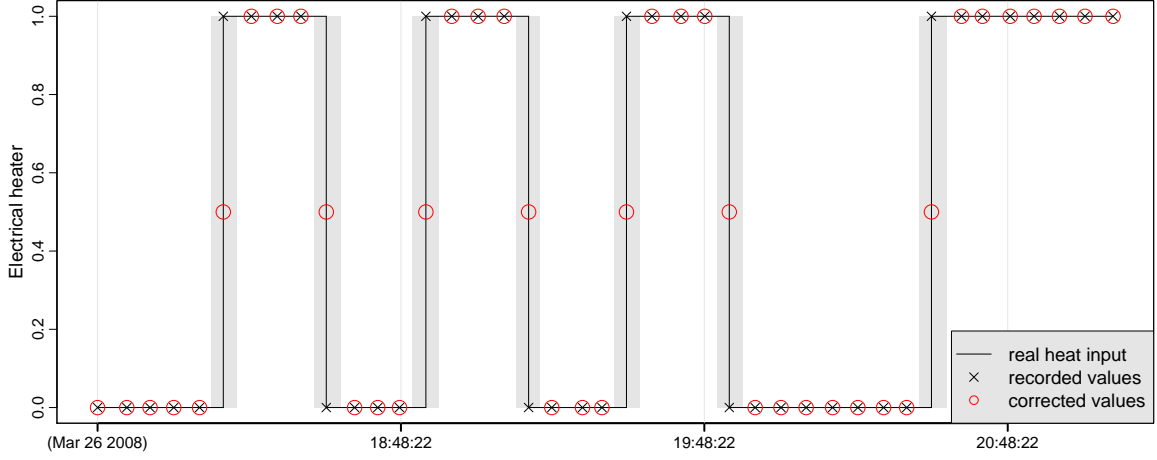


Figure 2.6: Correction of heater signal.

highest variance of the data and the second is parallel to the second highest variation etc. The axes in the new coordinate system are called the principal axes and are determined by the eigenvectors of the covariance matrix.

Consider n separate signals as a stochastic vector

$$\mathbf{X}_t = [X_t^1 \ X_t^2 \ \dots \ X_t^n]^T. \quad (2.2)$$

The ordered eigenvalues

$$\lambda_1 \leq \lambda_2 \leq \dots \leq \lambda_n \quad (2.3)$$

of the covariance matrix Σ for \mathbf{X}_t can be calculated using observations of the signals. The corresponding eigenvectors

$$\phi_1, \phi_2, \dots, \phi_n \quad (2.4)$$

can now be used to find the i 'th principal component

$$Y_{i,t} = \phi_i^T \mathbf{X}_t. \quad (2.5)$$

The proportion of variance explained by the i 'th principal component is

$$p_i = \frac{\lambda_i}{\sum_{i=1}^n \lambda_i} \quad (2.6)$$

where λ_i is the eigenvalue corresponding to the i 'th eigenvector.

The first principal component of the room temperatures is used as the indoor temperature T_i . The principal component analysis is carried out on all three experiments merged together. The eigenvector of the first principal component is found to

$$\phi_1 = [0.368 \ 0.406 \ 0.374 \ 0.371 \ 0.378 \ 0.392 \ 0.354]^T. \quad (2.7)$$

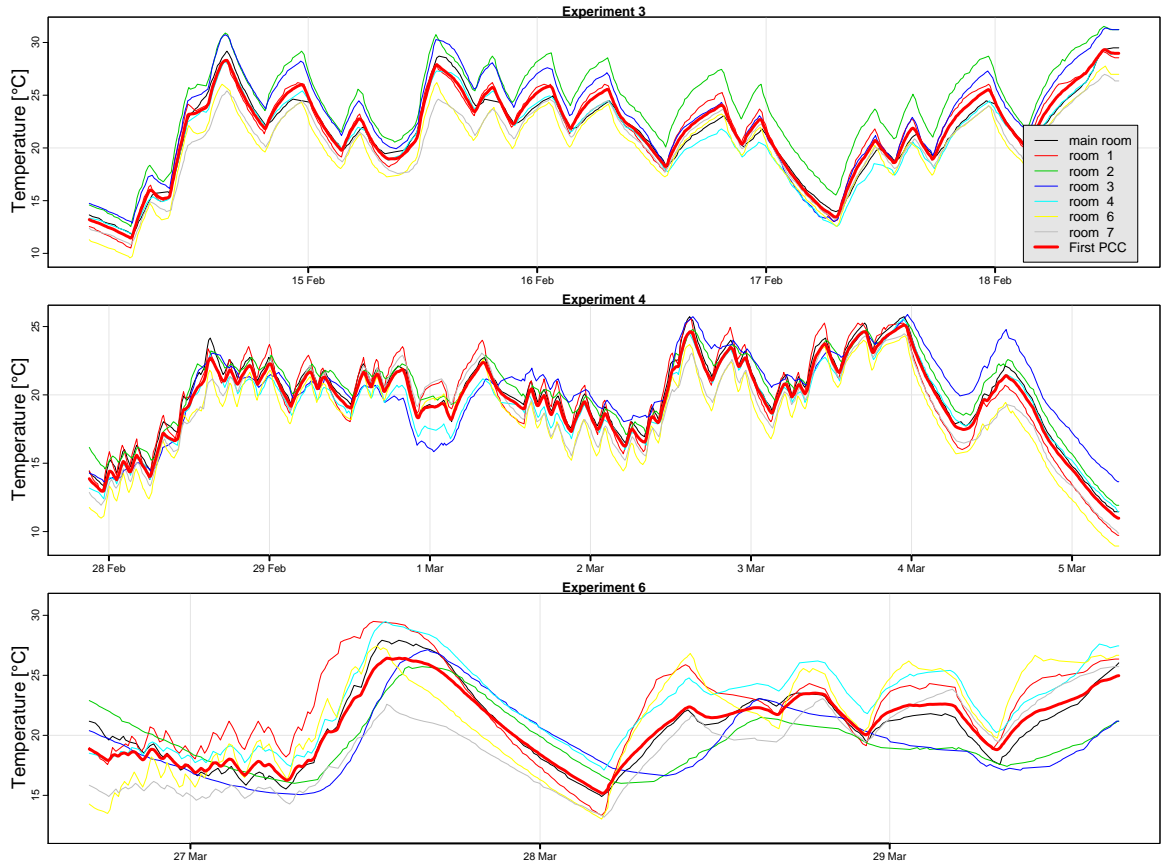


Figure 2.7: The temperatures in each room and the first principal component.

Since the range of the coefficients in ϕ_1 is relatively small, then the first principal component is very close to the average of the room temperatures. This indicates that variation of the room temperature signals are in equivalent. The three first proportions of variance are found to

$$\lambda_1 = 0.868 \quad (2.8)$$

$$\lambda_2 = 0.088 \quad (2.9)$$

$$\lambda_3 = 0.023. \quad (2.10)$$

Hence 86.8% of the variance is described by ϕ_1 , which closely resembles the mean. The high value of λ_1 indicate that the room temperatures that none of them are varying differently than the rest. The plot in Figure 2.7 show the temperatures in each room and first principal component.

Chapter 3

Models for the heat dynamics of a building

When modelling the heat dynamics of a building mainly two fundamental aspects are considered. That is, how the heat transfer between the building parts occur and by which entities of the building the model should be divided into. This chapter starts by outlining the theory of heat dynamics and the approximations made in the present models. In the last part of the chapter the grey-box modelling approach is described.

3.1 Heat dynamics

Theory of heat dynamics describes the transfer of thermal energy. Thermal energy is energy accumulated in a medium or object as movement of particles, and heat transfer is the transfer of thermal energy from an object to its surroundings. According to the second law of thermodynamics the thermal energy transfer is always towards the area with lower energy, i.e. in the direction of the negative temperature gradient. In this way the temperature is always equalized between an object and its surroundings.

3.1.1 Heat Capacity

The capability of a given entity, that is a physical medium or object, e.g. the air in a room or a wall in a building, to accumulate thermal energy is described by its heat capacity C . When heat Q , which is the transferred thermal energy is transferred to the object then the temperature T in the object changes. The heat capacity of the object as a function of the temperature is defined as

$$C(T) = mc(T) = \frac{dQ}{dT} \quad (3.1)$$

where m is the mass of the object, $c(T)$ is the specific heat capacity of the material in the object. The unit of C is $[\frac{J}{^\circ C}]$. In the present models T varies at normal room temperature

and the dependency of T is therefore marginal, and the linear approximation

$$C = \frac{dQ}{dT} \quad (3.2)$$

is used.

3.1.2 Heat Transfer

Heat transfer takes place via one of the following fundamental mechanisms

- conduction
- convection
- radiation

Heat transfer is always from areas of higher temperature toward areas of lower temperature and is in general a combination of the three stated mechanisms.

The heat transferred to a system per unit time is the heat flow

$$\frac{dQ}{dt} = C \frac{dT}{dt}. \quad (3.3)$$

where t is the time. This fundamental relation is utilized in the applied method as the link between a model of heat flows, which are not directly measured, and temperatures which are measured. Furthermore this makes it possible to estimate the heat capacities, since the models are formulated such that they are included as model parameters.

Conduction

When a homogeneous medium is conducting thermal energy, the heat conduction per area is proportional to the negative temperature gradient

$$\frac{1}{A} \frac{d\mathbf{Q}}{dt} = -\lambda \nabla T = -\lambda \left[\frac{dT}{dx}; \frac{dT}{dy}; \frac{dT}{dz} \right] \quad (3.4)$$

where A is the surface area through which the heat flows, λ is the thermal conductivity of the medium. The conductivity is in general dependent on several physical factors, e.g. temperature and moisture, but is in the present models assumed to be constant.

The change in temperature in the medium is described by the diffusion equation. When no heat sinks or sources exist in the conducting medium, the diffusion equation is given by

$$\frac{dT}{dt} = \frac{\lambda}{c\rho} \nabla^2 T = \frac{\lambda}{c\rho} \left(\frac{d^2T}{dx^2} + \frac{d^2T}{dy^2} + \frac{d^2T}{dz^2} \right) \quad (3.5)$$

where ρ is the density of the medium.

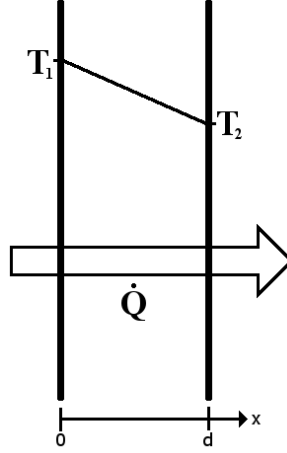


Figure 3.1: Heat transfer through a medium assuming a constant temperature gradient.

When heat flow through a wall is modelled in the present models, it is approximated to be in the normal direction of the wall only. This reduces the heat conduction per area to

$$\frac{1}{A} \frac{dQ}{dt} = -\lambda \frac{dT}{dx} \quad (3.6)$$

and the change in temperature to

$$\frac{dT}{dt} = \frac{\lambda}{c\rho} \frac{d^2T}{dx^2}. \quad (3.7)$$

Assuming a stationary condition of temperatures T_1 and T_2 , which are the temperatures on each side of the wall, then

$$\frac{dT}{dt} = 0 \Rightarrow \frac{d^2T}{dx^2} = 0 \Rightarrow \frac{dT}{dx} = a = \frac{T_2 - T_1}{L} \quad (3.8)$$

where a is some constant and L is the thickness of the wall. This is the heat conduction used in the present models and is illustrated in Figure 3.1.

Finally the relation between the temperatures on each side of a wall and the heat flow through the wall can be found from (3.6) and (3.8)

$$\frac{dQ}{dt} = \frac{\lambda A}{L} (T_1 - T_2) \quad (3.9)$$

which is the heat flow from side 1 to side 2. Since the models are formulated such that the heat flows between the entities in model are considered, disregarding the area and thickness of the wall, the R-values are used

$$\frac{dQ}{dt} = \frac{1}{R} (T_1 - T_2) \quad (3.10)$$

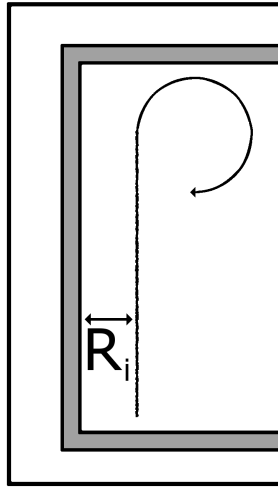


Figure 3.2: Resistance to heat flow by convection

where

$$R = \frac{L}{\lambda A} \quad (3.11)$$

is the resistance to heat flow between two entities, and has the unit $[\frac{^{\circ}\text{C}}{\text{W}}]$. Often the UA-values are used and this is simply the inverse of the R-value.

Convection

Convective heat transfer is a mechanism of heat transfer occurring because of bulk motion (observable movement) of fluids. As convection is dependent on the bulk movement of a fluid it can only occur in liquids, gases and multiphase mixtures. Convective heat transfer is split into two categories: natural (or free) convection and forced (or advective) convection, also known as heat advection

Heat transfer by convection is due to a combination of conduction and mass transfer. When a fluid is adjacent to a solid material, heat is transferred between them. If the fluid has a lower temperature than the solid, heat is transferred from the solid to the fluid by conduction. This increases the temperature of the fluid near the wall, which makes the fluid rise and this is replaced by new fluid. The opposite can also happen where warm fluid transfer heat to the solid which sinks down and is replaced by new fluid. The first example is illustrated in Figure 3.2.

As mentioned convection is divided into two categories

- Forced convection
- Free convection

Forced convection is the result of forced fluid flow, e.g. with fans or pumps. In free convection the fluid flows naturally due to density differences in the fluid. For the heat

transfer in FlexHouse only free convection will be regarded as a mechanism for exchanging heat between the indoor air and walls.

The heat flow by convection is given by Newton's law of cooling

$$\frac{dQ}{dt} = hA(T_s - T_\infty) \quad (3.12)$$

where h is the convection heat transfer coefficient, A is the area of the shared surface, T_s is the temperature of the solid and T_∞ is the temperature of the fluid far from the solid. A typical value of h is 2-to-25 W/(m² °C), for free convection of gases.

Convection can be modelled similarly to conduction, by setting $hA = 1/R$, where R is the resistance against heat transfer between the air and walls.

Radiation

Heat exchange by radiation occurs between all objects, having different temperature, that are in optical contact, e.g. radiation is the mode by which heat is transferred from the sun to the earth. The energy is emitted in the form of electromagnetic waves and therefore does not need a medium to propagate in. The energy emitted by a surface is given by

$$\frac{dQ}{dt} = \epsilon\sigma A_s T_s^4 \quad (3.13)$$

where ϵ is the emissivity of the surface, $\sigma = 5.670 \cdot 10^{-8}$ W/(m²K⁴) is Stefan-Boltzmann's constant, A_s is the area of the surface that radiates the energy and T_s is the surface temperature. In general heat transfer by radiation is very complex to calculate, since it involves integration over visible surfaces. The heat exchange, however, between a body and a totally surrounding surface can easily be calculated

$$\frac{dQ}{dt} = \epsilon\sigma A_s (T_s^4 - T^4) \quad (3.14)$$

The solar radiation has a big impact on the temperature inside buildings with windows and therefore solar radiation has to be a part of the heat transfer model. The heat flow through a window due to solar radiation can be described by

$$\frac{dQ}{dt} = A_w \Phi_s \quad (3.15)$$

where A_w is the effective window area and Φ_s is the outdoor solar radiation in W/m². The effective window area is equivalent to the area where the radiation can pass unimpeded.

Ventilation

Ventilation cause heat transfer due to mass transfer. For most old buildings, like Flex-House, the house envelope is by no means airtight and the indoor temperature is therefore

very dependent on the speed and direction of the wind. The total heat exchange due to ventilation is given by

$$\frac{dQ}{dt} = vc \quad (3.16)$$

where v is the amount of ventilated air and c is the specific heat capacity of air.

As with convection, ventilation can either be free or forced. For the heat transfer in FlexHouse only free ventilation is regarded as mode of exchanging heat between the indoor and outdoor air assuming that the air-conditioners are turned off. The amount of free ventilated air is very complex to calculate and depends on many factors, e.g. leakage area, wind speed and direction. Moreover the amount of ventilated air is by no means linear. In previous research conducted in FlexHouse [2] the following relation was proposed for the amount of ventilated air

$$v = \sum \left(A_1 \sqrt{A\Delta T + BV^2} \right) \quad (3.17)$$

where the sum is over all sides of the building, A_1 is the effective leakage area, A is the stack coefficient, B is the wind coefficient, V is the wind component and ΔT is the temperature difference between the indoor and the outdoor temperature.

Due to the age of FlexHouse, the house envelope cannot be assumed to be airtight. [2] estimates the heat loss, in FlexHouse, due to ventilation to be approximately 30% of the total heat loss. This heat loss has to be accounted for in the model of the heat flow. In [2] Equation 3.17 is approximated to be proportional to the temperature difference across the wall, i.e. ventilation loss can be approximated with

$$\frac{dQ}{dt} = k(T_i - T_a) = \frac{1}{R}(T_i - T_a) \quad (3.18)$$

where T_i is the indoor air temperature, T_a is the outdoor temperature and R is the resistance to heat transfer directly to the outside. This approximation holds for low wind speed, but if the wind speed is high ($> 5 \text{ m/s}$) the heat transfer becomes non-linear.

From this section it is seen that conduction, convection and ventilation, approximately, can be modeled as a resistances against heat transfer. The energy flow into the building due to direct solar radiation can be directly calculated using Equation 3.15 if the outdoor solar radiation is known.

3.2 Modelling Approach

When formulating a model for the heat dynamics of a building, three different approaches can be used. The most widespread approach is to formulate a deterministic physical model of the building with which the heat transfer can be simulated in different atmospheric conditions. This approach is called white-box or transparent modelling. A white-box model is continuously formulated. An overview of the vast amount of studies and computer software based on this approach can be found in [4]. Generally the white-box models require detailed building data, such as a 3D model of the dimensions of and the materials in the building.

The simple approach, in terms of physical information needed about the building, is black-box modelling. Here observed data, e.g. the outdoor temperature etc., is used as input to a statistically derived model of some variable e.g. the indoor temperature. A black-box model is discrete and thus contrary to a continuous white-box model. The advantage that little physical information about the building is needed, is also the disadvantage since that less interpretation of the underlying physical parameters can be achieved. Examples of black-box regression models where UA-values of single family houses are estimated can be found in [10]. The link between the grey-box models and the regression models is described in Section 3.4.

The approach used in the present models is grey-box modelling, which is a combination of white-box and black-box modelling. A grey-box model exploits the advantages of these two approaches by both including a continuous physical part and a discrete stochastic part.

3.3 Grey-box model

A grey-box model is a model established using a combination of prior physical knowledge and statistics, i.e. information embedded in data. The prior physical knowledge is described by a lumped model of the heat dynamics of the building, which is formulated as a deterministic linear state space model in continuous time. Since the model is lumped a noise term is added to describe the effects which is not described by the deterministic model. Thereby a stochastic linear state space model in continuous time is formed. The information embedded in the observed data is used for parameter estimation, by the formulation of a discrete measurement equation. Furthermore this enables evaluation and tests of the performance of the model. For example the dynamics that is not reflected by the model should optimally be white noise, indicating that the lumped model is consistent with the observed heat dynamics of the building.

3.3.1 Stochastic linear state space model

This section describes how the lumped model of the heat dynamics is formulated as a linear state space model, by the use of the heat dynamics theory described in Section 3.1. All the applied models approximate the interior of the building to be one room, and thus that variations of the indoor temperature within the building are close to zero in all areas. The state space model consists of: a set of state variables that describe the state of the system, a set of inputs that affects the system, and a set of continuous differential equations that describe the dynamics of the system. An RC-diagram of a linear model is depicted in Figure 3.3. The model has two heat capacities and two corresponding state variables. The heat flow between building parts are modelled as a combination of a conductive and a convective heat flow, which is simply characterised by a single thermal resistance, i.e. an R-value. Finally the stochastic linear state space model is formed by adding a noise term.

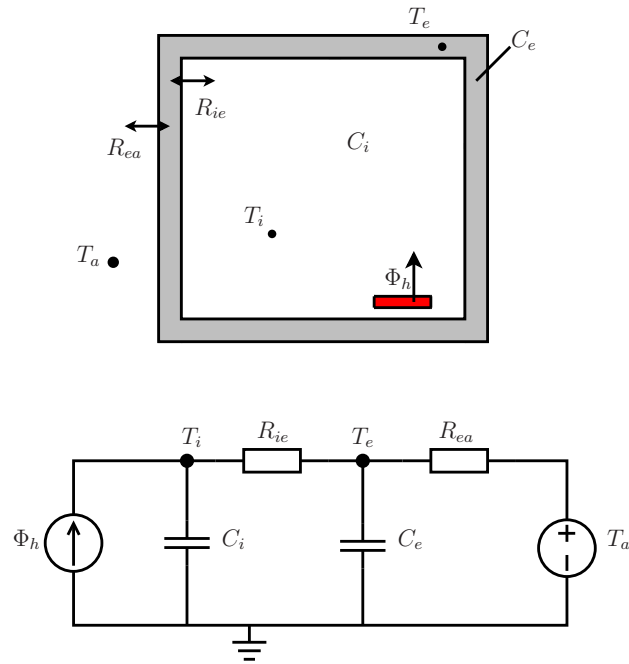


Figure 3.3: An RC-diagram and illustration of a lumped model of the heat dynamics of a building.

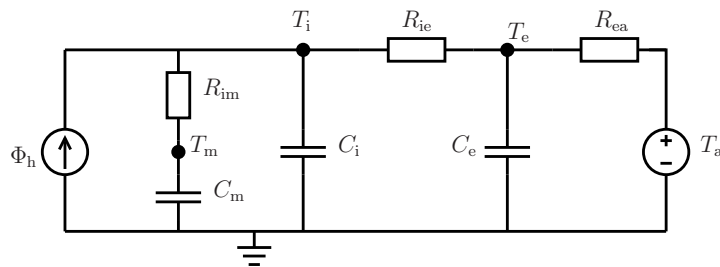


Figure 3.4: A linear model with three state variables.

State variables

The state variables of the model shown in Figure 3.3 are the indoor temperature T_i and the building envelope temperature T_e . Decreasing the number of state variables in the model makes it more lumped. Thus a less lumped model would include more state variables, e.g. the temperature in each room. In the model C_i represent the total heat capacity both of the indoor air and the interior walls etc. If one more state variable, and corresponding heat capacity and heat resistance, is added to the model, as in the model shown in Figure 3.4, then the heat capacity that is represented by C_i has changed. Thus it is seen that the physical interpretation of the parameters is dependent on how building is divided into

entities in the model.

Inputs

Measurements of physical variables are used as input to the state space models. The relevant inputs are those physical variables which affect the state of the system. The input variables of the model showed in Figure 3.3 are the ambient temperature T_a and the heat from the electrical heaters Φ_h .

Equations describing the heat dynamics

The dynamics of the lumped system is described by first order differential equations which can either be linear or non-linear. The differential equations are based on the heat dynamic theory. In the model showed in Figure 3.3, it is seen that the indoor temperature is dependent on two heat flows. The heat flow from the building envelope to the indoor air is modelled as a combination of a conductive and a convective heat flow. The heat flow from the electrical heater to the indoor air is simply given by Φ_h . This leads to the differential equation describing the first-order dynamics of indoor temperature

$$C_i \frac{dT_i}{dt} = \frac{1}{R_{ie}}(T_e - T_i) + \Phi_h \quad (3.19)$$

where R_{ie} is the thermal resistance between the building envelope and the indoor air.

The building envelope temperature also dependent on two heat flows, which are both modelled as a combination of a conductive and a convective heat flow. This leads to the first-order dynamics of the building envelope temperature

$$C_e \frac{dT_e}{dt} = \frac{1}{R_{ie}}(T_i - T_e) + \frac{1}{R_{ea}}(T_a - T_e). \quad (3.20)$$

where R_{ea} is the thermal resistance between the building envelope and the ambient environment.

Matrix form

The linear state space model depicted in Figure 3.3 on matrix form is

$$\begin{bmatrix} \frac{dT_i}{dt} \\ \frac{dT_e}{dt} \end{bmatrix} = \begin{bmatrix} \frac{-1}{C_i R_{ie}} & \frac{1}{C_i R_{ie}} \\ \frac{1}{C_e R_{ie}} & \frac{-1}{C_e} \left(\frac{1}{R_{ie}} + \frac{1}{R_{ea}} \right) \end{bmatrix} \begin{bmatrix} T_i \\ T_e \end{bmatrix} + \begin{bmatrix} 0 & \frac{1}{C_i} \\ \frac{1}{C_e R_{ie}} & \frac{-1}{C_e} \left(\frac{1}{R_{ie}} + \frac{1}{R_{ea}} \right) \end{bmatrix} \begin{bmatrix} T_a \\ \Phi_h \end{bmatrix} \quad (3.21)$$

and is written as

$$d\mathbf{T} = \mathbf{A}\mathbf{T}dt + \mathbf{B}\mathbf{U}dt \quad (3.22)$$

where $\mathbf{T} = [T_i, T_e]^T$ is the state vector and $\mathbf{U} = [T_a, \Phi_h]^T$ is the input vector. \mathbf{A} defines how the current state affects the dynamics and \mathbf{B} defines how input enters the system.

Noise term

To formulate a stochastic state space model, a noise term is added to the state space model. The state space models describes a deterministic system where future states can be precisely predicted if the input and the initial state vector are known. Due to approximations and unknown disturbances in the system this idealization cannot be assumed to be correct. Thus an additive noise term, $d\boldsymbol{\omega}(t)$ is introduced to form the stochastic linear state space model in continuous time

$$d\mathbf{T} = \mathbf{A}\mathbf{T}dt + \mathbf{B}Udt + d\boldsymbol{\omega}(t) \quad (3.23)$$

where $\boldsymbol{\omega}(t)$ is a Wiener process, which is a stochastic process with independent normal distributed increments.

3.3.2 Measurement equation

Unfortunately not all states that can be measured, e.g. the building envelope temperature. Therefore a vector of measurable states is introduced. This is defined by the discrete equation

$$\mathbf{T}_r = \mathbf{C}\mathbf{T} + \mathbf{D}U + \mathbf{e}(t) \quad (3.24)$$

where $\mathbf{e}(t)$ is the measurement error. It is assumed that $\mathbf{e}(t)$ is normal distributed white noise with zero mean and variance R_e . Furthermore it is assumed that $\mathbf{e}(t)$ and $\boldsymbol{\omega}(t)$ are mutually uncorrelated. \mathbf{C} and \mathbf{D} defines how the measured states are influenced by the state and input respectively. Considering the example model showed in Figure 3.3 it is seen that the input has no direct influence on the measured air temperature, and therefore $\mathbf{D} = \mathbf{0}$. \mathbf{C} is used to select the states which are measured. For all the models in the present study only the indoor air temperature is measured. The measurement equation for the example model is thus given by

$$T_r = [1 \ 0] \begin{bmatrix} T_i \\ T_e \end{bmatrix} + e(t) = T_i + e(t). \quad (3.25)$$

3.4 Link to regression models

The link between the state space models and the regression models considered in [10] for estimation of UA-values, is described in the following. Ignoring the dynamics by setting $\frac{dT_i}{dt}$ to zero, the simple state space model

$$C \frac{dT_i}{dt} = \frac{1}{R}(T_a - T_i) + \Phi_h \quad (3.26)$$

can be rewritten as

$$\begin{aligned} 0 &= \frac{1}{R}(T_a - T_i) + \Phi_h \Leftrightarrow \\ \Phi_h &= \frac{1}{R}(T_i - T_a). \end{aligned} \quad (3.27)$$

Then since the UA-value

$$\alpha_{\text{UA}} = \frac{1}{R} \quad (3.28)$$

and by adding a noise term, the model is

$$\Phi_{\text{h}} = \alpha_{\text{UA}}(T_{\text{i}} - T_{\text{a}}) + \epsilon. \quad (3.29)$$

This is the basis for the regression models in [10].

Chapter 4

Parameter estimation

In Chapter 3 a grey-box model of the heat dynamics of FlexHouse is formulated. This chapter describes a method for estimation of the parameters in the model, i.e. the thermal resistances and capacities etc. Furthermore it is showed how the time constants are computed and finally statistical tests applied in the model selection strategy is described.

In the first section it is described how the stochastic linear state space model in continuous time is transformed into discrete time. Then the maximum likelihood estimator used to estimate parameters is outlined, followed by a short description of CTSM, which is the software tool used for the calculations. Finally the computation of the time constants and the statistical tests used for the model selection strategy are described.

4.1 Stochastic linear state space model in discrete time

The stochastic linear state space model, described in Section 3.3.1, is formulated in continuous time, but the parameter estimation is carried out with statistical techniques applied to data, which is naturally measured in discrete time. The solution to the continuous stochastic differential equation (3.23) is found, such that the state of the system can be calculated for discrete time steps. The solution to (3.23) can analytically be found to

$$\begin{aligned} \mathbf{T}(t) = & \exp(\mathbf{A}(t - t_0))\mathbf{T}(t_0) + \int_{t_0}^t \exp(\mathbf{A}(t - s))\mathbf{B}\mathbf{U}(s)ds \\ & + \int_{t_0}^t \exp(\mathbf{A}(t - s))d\boldsymbol{\omega}(s) \end{aligned} \quad (4.1)$$

where

$$\exp(\mathbf{A}) = \sum_{k=0}^{\infty} \frac{1}{k!} \mathbf{A}^k = \mathbf{I} + \mathbf{A} + \frac{1}{2} \mathbf{A}^2 + \dots \quad (4.2)$$

See [5] for more details. Given the state vector at time t , $\mathbf{T}(t)$, the new state vector at time $t + \tau$ is given by

$$\begin{aligned}\mathbf{T}(t + \tau) &= \exp(\mathbf{A}(t + \tau - t))\mathbf{T}(t) + \int_t^{t+\tau} \exp(\mathbf{A}(t + \tau - s))\mathbf{B}\mathbf{U}(s)ds \\ &\quad + \int_t^{t+\tau} \exp(\mathbf{A}(t + \tau - s))d\boldsymbol{\omega}(s)\end{aligned}\quad (4.3)$$

Assuming that the input, $\mathbf{U}(t)$, is constant in the sample interval $[t; t + \tau]$, (4.3) can be reformulated to

$$\begin{aligned}\mathbf{T}(t + \tau) &= \exp(\mathbf{A}\tau)\mathbf{T}(t) - \int_\tau^0 \exp(\mathbf{A}r)\mathbf{B}dr\mathbf{U}(t) \\ &\quad + \int_t^{t+\tau} \exp(\mathbf{A}(t + \tau - s))d\boldsymbol{\omega}(s) \\ &= \exp(\mathbf{A}\tau)\mathbf{T}(t) + \int_0^\tau \exp(\mathbf{A}r)\mathbf{B}dr\mathbf{U}(t) \\ &\quad + \int_t^{t+\tau} \exp(\mathbf{A}(t + \tau - s))d\boldsymbol{\omega}(s)\end{aligned}\quad (4.4)$$

where the substitution $r = t + \tau - s$ has been used. Defining

$$\begin{aligned}\boldsymbol{\Phi}(\tau) &= \exp(\mathbf{A}\tau) \\ \boldsymbol{\Gamma}(\tau) &= \int_0^\tau \exp(\mathbf{A}r)\mathbf{B}dr \\ \mathbf{v}(t; \tau) &= \int_t^{t+\tau} \exp(\mathbf{A}(t + \tau - s))d\boldsymbol{\omega}(s)\end{aligned}\quad (4.5)$$

Then (4.4) can be written as

$$\mathbf{T}(t + \tau) = \boldsymbol{\Phi}(\tau)\mathbf{T}(t) + \boldsymbol{\Gamma}(\tau)\mathbf{U}(t) + \mathbf{v}(t, \tau)\quad (4.6)$$

Assuming that $\boldsymbol{\omega}(t)$ is a Wiener process, $\mathbf{v}(t; \tau)$ becomes normally distributed white noise with zero mean and covariance

$$\begin{aligned}\mathbf{R}_1(\tau) &= E[\mathbf{v}(t; \tau)\mathbf{v}(t; \tau)^T] = \int_0^\tau \boldsymbol{\Phi}(s)\mathbf{R}_1\boldsymbol{\Phi}(s)^T ds \\ &= \begin{bmatrix} R_{11} & 0 & 0 \\ 0 & R_{22} & 0 \\ 0 & 0 & R_{33} \end{bmatrix}\end{aligned}\quad (4.7)$$

If the sampling time is constant, the time scale in (4.6) can be transformed such that the sampling time is equal to one time unit, i.e.

$$\mathbf{T}(t + 1) = \boldsymbol{\Phi}\mathbf{T}(t) + \boldsymbol{\Gamma}\mathbf{U}(t) + \mathbf{v}(t)\quad (4.8)$$

This formulation can be used for estimation of the unknown parameters in (3.23) without losing the physical interpretation of the parameters.

4.2 Maximum Likelihood Estimator

In Section 4.1, it was found that the stochastic linear state space model in continuous time could be formulated as a difference equation in discrete time

$$\mathbf{T}(t+1) = \mathbf{\Phi}\mathbf{T}(t) + \mathbf{\Gamma}\mathbf{U}(t) + \mathbf{v}(t) \quad t \in 0, 1, 2, \dots, N \quad (4.9)$$

when the sampling time is constant, that is, equally spaced observations. In (4.9) t corresponds to the measurement at time index t , i.e. the t 'th measurement. The likelihood function can be used to estimate the unknown parameters in $\mathbf{\Phi}$ and $\mathbf{\Gamma}$, where the most likely estimator is given by

$$\hat{\boldsymbol{\theta}} = \arg \max_{\boldsymbol{\theta}} \{L(\boldsymbol{\theta}; \mathbf{T}_r(N))\} \quad (4.10)$$

where L , the likelihood function, is the joint probability distribution function of all the observations.

Let $\mathbf{T}_r(t) = [T_r(t), T_r(t-1), \dots, T_r(0)]$ be a vector containing all observations up to and including t and $\boldsymbol{\theta}$ be a vector containing all the unknown parameters in $\mathbf{\Phi}$ and $\mathbf{\Gamma}$, including R_{11} , R_{22} , R_{33} from (4.7) and the measurement error, R_e . Then the likelihood function can be formulated as the joint probability distribution when $\boldsymbol{\theta}$ is given

$$\begin{aligned} L(\boldsymbol{\theta}; \mathbf{T}_r(N)) &= p(\mathbf{T}_r(N)|\boldsymbol{\theta}) \\ &= p(\mathbf{T}_r(N)|\mathbf{T}_r(N-1), \boldsymbol{\theta})p(\mathbf{T}_r(N-1)|\boldsymbol{\theta}) \\ &= \left(\prod_{t=1}^N p(\mathbf{T}_r(t)|\mathbf{T}_r(t-1), \boldsymbol{\theta}) \right) p(\mathbf{T}_r(0)|\boldsymbol{\theta}) \end{aligned} \quad (4.11)$$

where the rule $P(A \cap B) = P(A|B)P(B)$ has been used N -times to form the likelihood function as a product of conditional densities. Since both $\mathbf{v}(t)$ and $e(t)$, in (4.8) and (3.24), are assumed to be normally distributed, the conditional density function is also normally distributed, and is thus fully characterized by its mean and variance. The multivariate normal distribution is given by

$$f(\mathbf{x}) = \frac{1}{(2\pi)^{n/2} \sqrt{\det \boldsymbol{\Sigma}}} \exp \left(-\frac{1}{2} (\mathbf{x} - \boldsymbol{\mu})^T \boldsymbol{\Sigma}^{-1} (\mathbf{x} - \boldsymbol{\mu}) \right) \quad (4.12)$$

where $\boldsymbol{\Sigma} > \mathbf{0}$ is the covariance and $\boldsymbol{\mu}$ is the mean. Introducing the conditional mean

$$\hat{\mathbf{T}}(t|t-1) = E[\mathbf{T}_r(t)|\mathbf{T}_r(t-1), \boldsymbol{\theta}] \quad (4.13)$$

the conditional variance

$$\mathbf{R}(t|t-1) = V[\mathbf{T}_r(t)|\mathbf{T}_r(t-1), \boldsymbol{\theta}] \quad (4.14)$$

and the one step prediction error

$$\boldsymbol{\varepsilon}(t) = \mathbf{T}(t) - \hat{\mathbf{T}}(t|t-1) \quad (4.15)$$

Then (4.11) can be reformulated to

$$L(\boldsymbol{\theta}; \mathbf{T}_r(N)) = \prod_{t=1}^N \left(\frac{1}{(2\pi)^{n/2} \sqrt{\det \mathbf{R}(t|t-1)}} \exp \left(-\frac{1}{2} \boldsymbol{\varepsilon}(t)^T \mathbf{R}(t|t-1)^{-1} \boldsymbol{\varepsilon}(t) \right) \right)$$

where n is the dimension of \mathbf{T}_r . To simplify the maximization the logarithm to the likelihood function is maximized instead

$$\begin{aligned} l(\boldsymbol{\theta}; \mathbf{T}_r(N)) &= \log \left(\prod_{t=1}^N \left(\frac{1}{(2\pi)^{n/2} \sqrt{\det \mathbf{R}(t|t-1)}} \exp \left(-\frac{1}{2} \boldsymbol{\varepsilon}(t)^T \mathbf{R}(t|t-1)^{-1} \boldsymbol{\varepsilon}(t) \right) \right) \right) \\ &= -\frac{m}{2} \sum_{t=1}^N (2\pi) - \frac{1}{2} \sum_{t=1}^N \log(\det \mathbf{R}(t|t-1)) + \frac{1}{2} \boldsymbol{\varepsilon}(t)^T \mathbf{R}(t|t-1)^{-1} \boldsymbol{\varepsilon}(t) \\ &= \frac{1}{2} \sum_{t=1}^N [\boldsymbol{\varepsilon}(t)^T \mathbf{R}(t|t-1)^{-1} \boldsymbol{\varepsilon}(t) - \log(\det \mathbf{R}(t|t-1))] + C \end{aligned} \quad (4.16)$$

where C is a constant. A Kalman filter can be applied to recursively calculate the conditional mean and variance.

The Kalman filter is a recursive filter, which can be used to estimate the states of a linear stochastic state space model, given observations of \mathbf{U} and \mathbf{T} . The reconstructed states and the corresponding covariance are

$$\hat{\mathbf{T}}(t|t) = \hat{\mathbf{T}}(t|t-1) + \mathbf{K}_t \left(\mathbf{T}_r(t) - \mathbf{C} \hat{\mathbf{T}}(t|t-1) \right) \mathbf{P}(t|t) = \mathbf{P}(t|t-1) - \mathbf{K}_t \mathbf{R}(t|t-1) \mathbf{K}_t^T$$

where \mathbf{K}_t is the Kalman gain given by

$$\mathbf{K}_t = \mathbf{P}(t|t-1) \mathbf{C}^T \mathbf{R}(t|t-1)^{-1} \quad (4.18)$$

The predicted states are given by

$$\begin{aligned} \hat{\mathbf{T}}(t+1|t) &= \boldsymbol{\Phi} \hat{\mathbf{T}}(t|t) + \boldsymbol{\Gamma} \mathbf{U}(t) \\ \hat{\mathbf{T}}_r(t+1|t) &= \mathbf{C} \hat{\mathbf{T}}(t+1|t) \\ \mathbf{P}(t+1|t) &= \boldsymbol{\Phi} \mathbf{P}(t|t) \boldsymbol{\Phi}^T + \mathbf{R}_1 \\ \mathbf{R}(t+1|t) &= \mathbf{C} \mathbf{P}(t+1|t) \mathbf{C}^T + \mathbf{R}_2 \end{aligned}$$

where following initial conditions are used

$$\begin{aligned} \hat{\mathbf{T}}(1|0) &= E[\mathbf{T}(1)] = \boldsymbol{\mu}_0 \\ \mathbf{P}(1|0) &= V[\mathbf{T}(1)] = \mathbf{V}_0 \end{aligned}$$

Asymptotically it holds for the maximum likelihood estimator that the variance of the estimate is given by

$$V[\hat{\boldsymbol{\theta}}] = \mathbf{I}^{-1}(\hat{\boldsymbol{\theta}}) \quad (4.19)$$

where

$$\mathbf{I}(\boldsymbol{\theta}) = -E \left[\frac{\partial^2 \log L}{\partial \boldsymbol{\theta}^2} \right] \quad (4.20)$$

In practice

$$\mathbf{I}(\boldsymbol{\theta}) = - \left[\frac{\partial^2 \log L}{\partial \boldsymbol{\theta}^2} \right]_{\boldsymbol{\theta}=\hat{\boldsymbol{\theta}}} \quad (4.21)$$

is used. From this the variance and p-value for the parameters are found.

4.3 CTSM - Continuous Time Stochastic Modeling

A routine for maximizing the conditional likelihood function has been implemented in CTSM, which is a continuous time stochastic modelling tool. CTSM can be used to estimate parameters in both linear time invariant-, linear time varying- and nonlinear models. The estimated parameters can either be found using the maximum likelihood (ML) method or the maximum a posteriori (MAP) method. The maximum a posteriori estimator is not used in this project, but [5] contains more information. When the maximum likelihood estimator has been found for $L(\mathbf{T}_r(N); \boldsymbol{\theta})$ CTSM returns the estimate of $\boldsymbol{\theta}$.

CTSM also estimates the standard deviation of the estimated parameters. This is given by the estimated variance, which is found by setting the expected value in (4.20) equal to the observed value, i.e.

$$i_{lk} = - \left(\frac{\partial^2 \log L(\boldsymbol{\theta}; \mathbf{T}_r(N);)}{\partial \theta_l \partial \theta_k} \right) \quad (4.22)$$

CTSM has been developed at Department of Informatics and Mathematical Modeling (IMM) at the Technical University of Denmark, (DTU), and can be downloaded from IMM's homepage ¹, where a user's guide [6] is also available.

4.3.1 Modelling in CTSM

Due to the ease of use, CTSM has been chosen for estimation of the parameters in (3.23). When a model, of the same form as (4.8), has been formulated it can easily be entered using the graphical user interface of CTSM. When the number of states, input and output have been defined, CTSM sets up the matrices, \mathbf{A} , \mathbf{B} , \mathbf{C} and \mathbf{D} , defined in (3.23) and (3.24). When the matrices have been filled out it can be selected how to estimate each parameter, i.e. ML, MAP or if it is fixed. Boundaries are defined for each parameter that

¹<http://www2.imm.dtu.dk/~ctsm/>

is to be estimated. It should be noted, that $\pm\infty$ and 0 should be avoided as boundary and initial values for the parameter estimation. Finally a source of data, which contain time, input and measured output, is specified and the parameters are estimated.

4.4 Time constants

Time constants characterizes the frequency response of a system. Physically, a single time constant represents the time it takes the system's step response to reach approximately 63% of its final (asymptotic) value. The i 'th time constant of a linear state space model is

$$\tau_i = -\frac{1}{\lambda_i} \quad (4.23)$$

where λ_i is the i 'th largest eigenvalue of \mathbf{A} defined in (3.22).

4.5 Tests for model expansion

Statistical tests that can be utilized in the search for the most appropriate model are useful. If a model is a submodel of larger model then a likelihood ratio test can determine if the larger model performs significantly better than the submodel. Using such tests a strategy for selection of the best model can be evolved.

4.5.1 Likelihood ratio tests

Let a model have parameters $\theta \in \Omega_1$ where $\Omega_1 \in \mathbb{R}^r$ is the parameter space and $r = \dim(\Omega_1)$ is the number of parameters in the model. Let a larger model have parameters $\theta \in \Omega_0$ where $\Omega_0 \in \mathbb{R}^m$ and $\dim(\Omega_0) = m$, and

$$\Omega_1 \subset \Omega_0, \quad (4.24)$$

i.e. the first model is a submodel of the second model and $r < m$.

The likelihood ratio test

$$\lambda(y) = \frac{\sup_{\theta \in \Omega_1} L(\theta; y)}{\sup_{\theta \in \Omega_0} L(\theta; y)} \quad (4.25)$$

where y is the observed values, can then be used to test the hypothesis

$$H_0 : \theta \in \Omega_1 \quad \text{vs.} \quad H_1 : \theta \notin \Omega_1, \quad (4.26)$$

since under H_0 the test statistic $-2\log(\lambda(y))$ converges to a χ^2 distributed random variable with $(m - r)$ degrees of freedom as the number of samples in y goes to infinity. If H_0 is rejected then the likelihood of the larger model is significant compared to the likelihood of the submodel, and it is found that y is more likely to be observed with the larger model. In words the H_0 hypothesis can be formulated as: can the optimal model have $\theta \in \Omega_1$? This can be rejected if a better model which have $\theta \in \Omega_0$ is found. For more details see [12].

4.5.2 Hypothesis chains

Having multiple models with parameters $\theta \in \Omega_i$ where

$$\mathbb{R} = \Omega_m \subset \dots \subset \Omega_1 \subset \Omega_0 \subset \mathbb{R}^k \quad (4.27)$$

and corresponding hypothesis

$$H_i^0 : \theta \in \Omega_i \quad \text{vs.} \quad H_i^1 : \theta \notin \Omega_i, \quad (4.28)$$

then

$$H_m \subset \dots \subset H_1 \subset H_0 \subset H_k \quad (4.29)$$

and

$$\neg H_i^0 \Rightarrow \neg H_{i+1}^0 \Rightarrow \dots \Rightarrow \neg H_m^0. \quad (4.30)$$

This means that if H_i^0 is rejected when testing a model against a submodel where parameters are removed, or set to zero, then it can be concluded that no submodel of this submodel is the optimal model. This can be used to test whether any submodel of a given model is significantly better than the model. It is simply needed to test each submodel where only a single parameter has been removed from the model.

Chapter 5

Linear models

Grey-box models applied to model the heat dynamics of FlexHouse are described in this chapter. The modelling procedure is first to apply a small model with only one state variable, and thus only one time constant, and then stepwise expand the model in a forward selection procedure. This is done until no further significant parameters and state variables can be added to the model. The likelihood ratio test is used to find a significant expansion of the model in each step.

The outline of the chapter is such that first the models which are selected in each step are described and finally the forward selection with the likelihood ratio test results is described.

5.1 Selected models

This section describes the selected linear models. The linear models can all be written

$$d\mathbf{T} = \mathbf{A}\mathbf{T}dt + \mathbf{B}\mathbf{U}dt + d\boldsymbol{\omega}(t) \quad (5.1)$$

where \mathbf{T} is the state vector and \mathbf{U} is the input vector, and none of the state variables or input variables are in \mathbf{A} or \mathbf{B} which only consist of parameters. All the considered linear models have an input vector with three inputs

$$\mathbf{U} = [T_a, \Phi_s, \Phi_h]^T. \quad (5.2)$$

where

- T_a is the temperature of the ambient environment, i.e. the outdoor air temperature,
- Φ_s is the solar irradiance on the building,
- Φ_h is the heat from the electrical heaters inside the building.

A description of the models are given from a theoretical point of view, but since the models are lumped these descriptions does not hold exactly when the models are applied. This is

elaborated further in Chapter 7 where the results of applying the models are presented. Furthermore it should be kept in mind these models are linear approximations to the real system.

5.1.1 Linear A

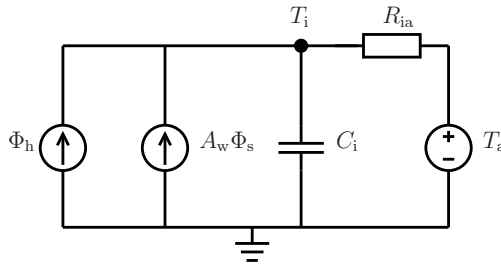


Figure 5.1: The Linear A model

The smallest applied model is denoted Linear A. The RC-network of Linear A is shown in Figure 5.1. The model has one state variable T_i which is the measured indoor temperature, and the following physical parameters

- C_i is the heat capacity of the house. This includes the indoor air, the interior objects, and the building envelope.
- R_{ia} is the thermal resistance from the indoor to the ambient environment.
- A_w is the effective window area of the house (see Section 3.1.2).

The differential equation describing the heat flow in the model is given by the heat flow to the indoor

$$C_i \frac{dT_i}{dt} = \frac{1}{R_{ia}}(T_a - T_i) + A_w \Phi_s + \Phi_h. \quad (5.3)$$

5.1.2 Linear B

The RC-network of Linear B is shown in Figure 5.2. The expansion from Linear A is obtained by adding a part that enhance the model of the heat input from the electrical heaters. This part describes the finding that there is a delay from turning on the heaters until this heat affects T_i . A state variable T_h representing the temperature in electrical heaters is added together with the following parameters

- C_h is the heat capacity of the electrical heaters,
- R_{ih} is the thermal resistance from the heaters to the indoor.

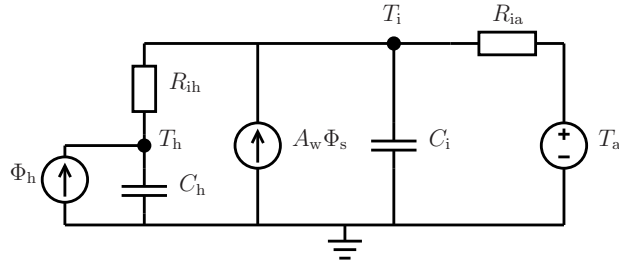


Figure 5.2: The Linear B model

It is also noted that expanding from a model with one heat capacity of the house, into a model with two heat capacities of the house, implies that the interpretation of the heat capacity parameters change. The model has two state variables $\mathbf{T} = [T_i, T_h]^T$, and the differential equations describing the heat flows in the model are:

$$C_i \frac{dT_i}{dt} = \frac{1}{R_{ia}}(T_a - T_i) + \frac{1}{R_{ih}}(T_h - T_i) + A_w \Phi_s \quad (5.4)$$

$$C_h \frac{dT_h}{dt} = \frac{1}{R_{ih}}(T_i - T_h) + \Phi_h. \quad (5.5)$$

5.1.3 Linear C

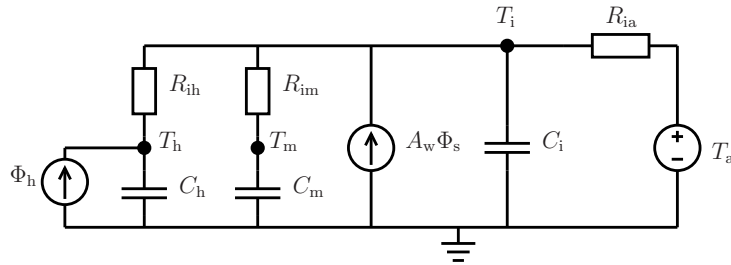


Figure 5.3: The Linear C model

The RC-network of Linear C is shown in Figure 5.3. The model is an expansion of Linear B, where a part that allows the indoor of the building to have one more separate medium. The state variable added is T_m and the extra parameters are

- C_m a second indoor heat capacity,
- R_{im} which is thermal resistance between the indoor and the second indoor medium.

The model has three state variables $\mathbf{T} = [T_i, T_m, T_h]^T$. The differential equations describing the heat flows in the model are

$$C_i \frac{dT_i}{dt} = \frac{1}{R_{ia}}(T_a - T_i) + \frac{1}{R_{im}}(T_m - T_i) + \frac{1}{R_{ih}}(T_h - T_i) + A_w \Phi_s \quad (5.6)$$

$$C_m \frac{dT_m}{dt} = \frac{1}{R_{im}}(T_i - T_m) \quad (5.7)$$

$$C_h \frac{dT_h}{dt} = \frac{1}{R_{ih}}(T_i - T_h) + \Phi_h \quad (5.8)$$

5.1.4 Linear D

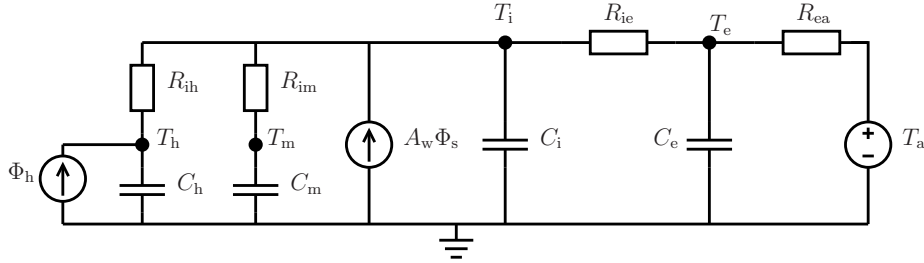


Figure 5.4: The Linear D model

The RC-network of Linear D is shown in Figure 5.4. This is an expansion of Linear C, where the description of the building envelope is enhanced. This is done by adding the state variable T_e which is the temperature in the building envelope. Correspondingly the following is added

- C_e is the heat capacity of the building envelope
- R_{ie} is the thermal resistance from the indoor to the building envelope
- R_{ea} is the thermal resistance from the building envelope to the ambient environment.

It is seen that R_{ia} is the part of Linear B which is replaced with an enhanced part. The model has four state variables $\mathbf{T} = [T_i, T_m, T_e, T_h]^T$. The differential equations describing

the heat flows in the model are

$$C_i \frac{dT_i}{dt} = \frac{1}{R_{ie}}(T_e - T_i) + \frac{1}{R_{im}}(T_m - T_i) + \frac{1}{R_{ih}}(T_h - T_i) + A_w \Phi_s \quad (5.9)$$

$$C_m \frac{dT_m}{dt} = \frac{1}{R_{im}}(T_i - T_m) \quad (5.10)$$

$$C_e \frac{dT_e}{dt} = \frac{1}{R_{ie}}(T_i - T_e) + \frac{1}{R_{ea}}(T_a - T_e) \quad (5.11)$$

$$C_h \frac{dT_h}{dt} = \frac{1}{R_{ih}}(T_i - T_h) + \Phi_h \quad (5.12)$$

5.1.5 Linear E

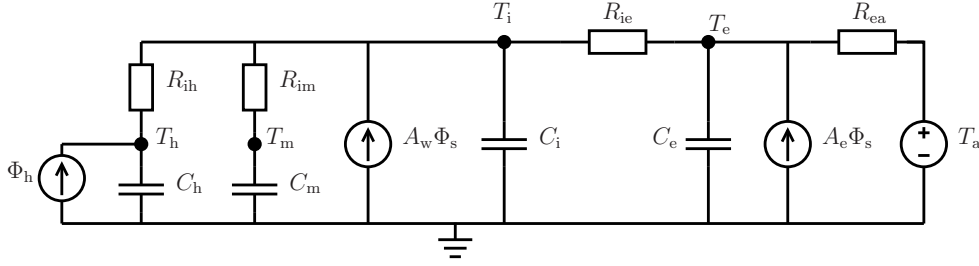


Figure 5.5: The Linear E model

The RC-network of Linear E is shown in Figure 5.5. This is the largest model applied and no significant further expansion was found possible. The expansion from Linear D is accomplished by allowing the solar energy to enter the building envelope. Hence one parameter is added

- A_e is the effective area in which the solar radiation enters.

The model has four state variables $\mathbf{T} = [T_i, T_m, T_e, T_h]^T$. The differential equations are

$$C_i \frac{dT_i}{dt} = \frac{1}{R_{ie}}(T_e - T_i) + \frac{1}{R_{im}}(T_m - T_i) + \frac{1}{R_{ih}}(T_h - T_i) + A_w \Phi_s \quad (5.13)$$

$$C_m \frac{dT_m}{dt} = \frac{1}{R_{im}}(T_i - T_m) \quad (5.14)$$

$$C_e \frac{dT_e}{dt} = \frac{1}{R_{ie}}(T_i - T_e) + \frac{1}{R_{ea}}(T_a - T_e) + A_e \Phi_s \quad (5.15)$$

$$C_h \frac{dT_h}{dt} = \frac{1}{R_{ih}}(T_i - T_h) + \Phi_h \quad (5.16)$$

5.2 Model selection

This section describes the selection of models using the likelihood ratio tests described in Section 4.5.1. First a small and simple model is chosen as a starting point for the selection and it is then expanded stepwise. The expansion in each step is either done by adding a new physical parameter or by adding a new state variable with corresponding physical parameters. In each step several expansions are tested and the most significant expansion is selected, which is accomplished by taking the expansion with the highest loglikelihood.

5.2.1 From Linear A to Linear B

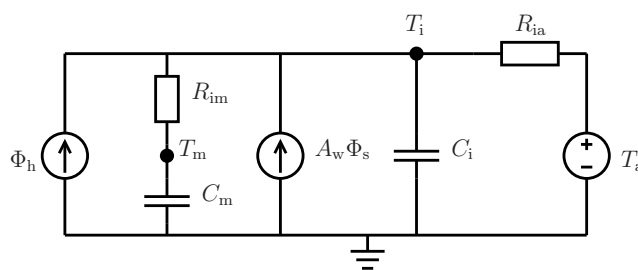


Figure 5.6: The Linear A model expanded with T_m

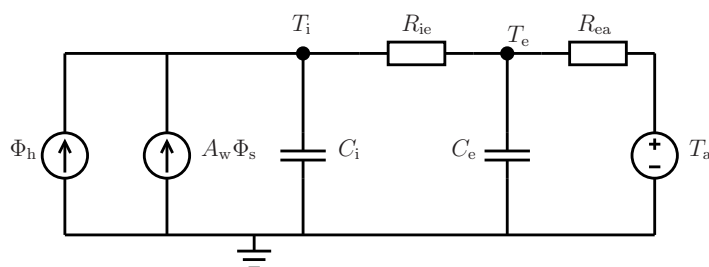


Figure 5.7: The Linear A model expanded with T_e

In this section is described how it is concluded that Linear B is the best one-step improvement compared to Linear A. Linear A (see p. 33, is the smallest reasonable model with the three inputs and one state variable and is therefore the smallest considered model. Three possible expansions into a model which has two state variables are evaluated and the most significant expansion is selected. An expansion with T_m as shown in Figure 5.6 gives

$$l(\theta; y) = 6627.8. \quad (5.17)$$

An expansion with T_e as shown in Figure 5.7 gives

$$l(\theta; y) = 6656.8. \quad (5.18)$$

It is seen that these two expansions gives almost the same value of the loglikelihood function. The third evaluated expansion is with T_h and is selected as Linear B (see p. 33), since this gives a loglikelihood of

$$l(\theta; y) = 6960.6. \quad (5.19)$$

Since all three expansions has expands with 4 parameters the most significant expansion is with T_h .

The test for significant difference between Linear A and Linear B is carried out by calculation of the likelihood ratio test statistic

$$\lambda = -2\log(e^{l(\theta_A)-l(\theta_B)}) = -2\log(e^{(5542.6-6960.6)}) = 4091.4 \quad (5.20)$$

which under H_0 follows a $\chi^2(10 - 6)$ distribution. The p-value is very close to zero and H_0 is rejected. It is thus found that Linear B is a significantly better model than Linear A.

5.2.2 From Linear B to Linear C

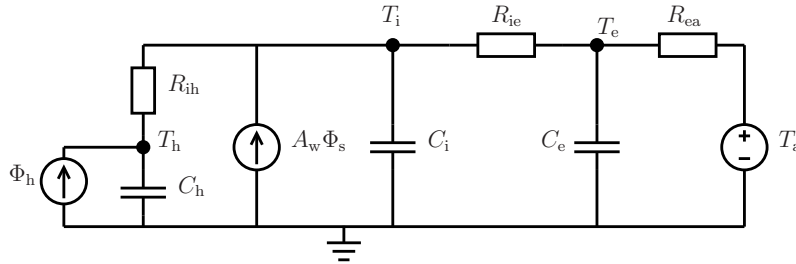


Figure 5.8: The Linear B model expanded with T_e

The expansion from Linear B to a larger model is done by testing two expansions. With T_e , as depicted in Figure 5.8, the loglikelihood function is

$$l(\theta; y) = 7245.6 \quad (5.21)$$

and with T_m

$$l(\theta; y) = 7254.0. \quad (5.22)$$

The expansion with T_m is selected as Linear C. The test for significant difference performance between Linear B and Linear C, is done by calculating

$$\lambda = -2\log(e^{(6960.6-7254.0)}) = 846.8 \quad (5.23)$$

which under H_0 follows a $\chi^2(14 - 10)$ distribution. The p-value of the test is approximately zero and thus H_0 is rejected. Hence it is concluded that the expansion is significant.

5.2.3 From Linear C to Linear D

The expansion from Linear C to Linear D is tested by calculating

$$\lambda = -2\log(e^{l(\theta_C)-l(\theta_D)}) = -2\log(e^{(7254.0-7551.1)}) = 857.4 \quad (5.24)$$

which under H_0 follows a $\chi^2(18 - 14)$ distribution. The p-value is approximately zero and H_0 is rejected. It is thus concluded that Linear D is significantly better than Linear C.

5.2.4 From Linear D to Linear E

The expansion from Linear D to Linear E is tested by calculating

$$\lambda = -2\log(e^{l(\theta_D)-l(\theta_E)}) = -2\log(e^{(7551.1-7610.7)}) = 171.7 \quad (5.25)$$

which under H_0 follows a $\chi^2(19 - 18)$ distribution. The p-value is close to 0 and H_0 is rejected. It is thus concluded that the expansion from Linear D to Linear E should be made.

5.3 Tests of expansions and submodels of Linear E

In this section it is described how to conclude that Linear E is the best model, currently found. First tests for further expansion of Linear E are carried out. An expansion of Linear E, where the solar radiation energy is splitted with a p -part flowing into the T_m entity and $(1 - p)$ into the T_i entity, is tested. The statistic is

$$\lambda = -2\log(e^{(7610.7-7611.2)}) = 1.62 \quad (5.26)$$

which under H_0 follows a $\chi^2(20 - 19)$ distribution. The p-value is 0.20 and H_0 cannot be rejected and it is concluded that this expansion should not be made.

An expansion with R_{ia} is tested by

$$\lambda = -2\log(e^{(7610.7-7612.0)}) = 3.94 \quad (5.27)$$

which under H_0 follows a $\chi^2(20 - 19)$ distribution. The p-value is 0.047, which is in a strict sense significant, but it is found that the improvement is too small and thus that the expansion should not be made. From this it is seen that no significant expansion currently has been found.

By testing all submodels where only one parameter, or for the present models the smallest possible part, has been removed, it can be tested if any submodel is significantly better than Linear E. See the details in Section 4.5.2. Therefore a test of removing T_m, C_m, R_{im} from Linear E is carried out and then a test of removing T_h, C_h, R_{ih} is carried out. This, together with the test of expansion from Linear D to Linear E, where A_e was added, is found sufficient to cover all submodels.

The test for removing T_m, C_m, R_{im} is carried out by calculating

$$\lambda = -2\log(e^{(6466.4-7612.0)}) = 3301.7 \quad (5.28)$$

which under H_0 follows a $\chi^2(19 - 15)$ distribution. The p-value is close to zero, and it concluded that the submodel is less significant.

The for removing T_h, C_h, R_{ih} is carried out by calculating

$$\lambda = -2\log(e^{(7279.5-7612.0)}) = 955.5 \quad (5.29)$$

which under H_0 follows a $\chi^2(19 - 15)$ distribution. The p-value is close to zero, and it concluded that the submodel is less significant.

From these tests it is found that no submodel or expansion of Linear E is significantly better than Linear E, and thereby that Linear E is the best model to describe the present data.

Chapter 6

Analysis of the one-step prediction error

For each selected model an analysis of the one-step prediction error

$$\epsilon_t = T_t^i - \hat{T}_{t|t-1}^i \quad (6.1)$$

where T_t^i is the observed indoor temperature at time t , is carried out. The one-step prediction error is in the following just referred to as the error. The aim of this analysis is to find how close the applied model is to the real model of the system. First the moments of the distribution of the error are used as performance measures for the models. Then the time series $\{\epsilon_t\}$ of observed errors is plotted together with the input signals $\{T_t^i\}$, $\{\Phi_t^s\}$, $\{\Phi_t^h\}$ and investigated to find which effects influence the performance of the models. Finally two statistics are calculated: the ACF and the cumulated periodogram, see [8]. These are plotted with a 95% confidence band, which is used to test if ϵ is white noise. This is of interest since if the applied model is the real model then the error will be white noise. Furthermore especially the ACF can give information of the shortcomings of the model. For all the calculated statistics a burn-in period of one hour for each experiment is used, i.e. they are calculated without the values of the first hour of each experiment.

6.1 Mean and variance of the one-step prediction error distribution

Name	Linear A	Linear B	Linear C	Linear D	Linear E
μ_ϵ	-0.000381	0.000358	0.000606	0.000594	8.28e-05
σ_ϵ^2	0.00274	0.000865	0.000724	0.000719	0.000691

Table 6.1: Moments of the distribution of the errors

The first two moments, the mean and the variance, of the distribution of ϵ are good performance measures of the models. The estimated values for each model are listed in Table 6.1. The mean is an estimate of the bias, and are in the same range from Linear A to Linear D, but is considerable smaller for Linear E. The variance is similarly decreasing, and it is seen that the performance is increasing in each step from Linear A to Linear E. The results are thus in agreement with the model selection carried out.

6.2 Linear A

Plot of the error for Linear A is found in Figure 6.1(a). Clearly the error has non-stationarities indicating that the optimal model is more flexible than Linear A, and thus should have more than one state variable and correspondingly more than one time constant. The variance of the error is expected to be higher in a period after the state of heaters is shifted. This is due to the higher differential of the indoor temperature after such a shift and thus a higher variance of the one-step prediction. It is seen that the error has a higher variance when the state of the heaters has shifted, but non-stationarities are also higher. The ACF of the error is plotted in Figure 6.1(b) together with the periodogram. High correlations of the lags are found and a high deviation from the 95% confidence band of white noise.

6.3 Linear B

Examining the plot of the error for Linear B in Figure 6.2(a) less non-stationarity is found comparing with Linear A. Especially around the state shifts of the heaters, for example this is clearly seen after the shift around 1036 hours. The variance of the error is higher after a shift, but as explained above this is expected. The plot of the ACF in Figure 6.2(b), shows a considerable decrease compared with ACF from Linear A. Similarly the periodogram is closer to the confidence band of white noise, and it is seen that the model clearly has improved the description of the high frequencies.

6.4 Linear C

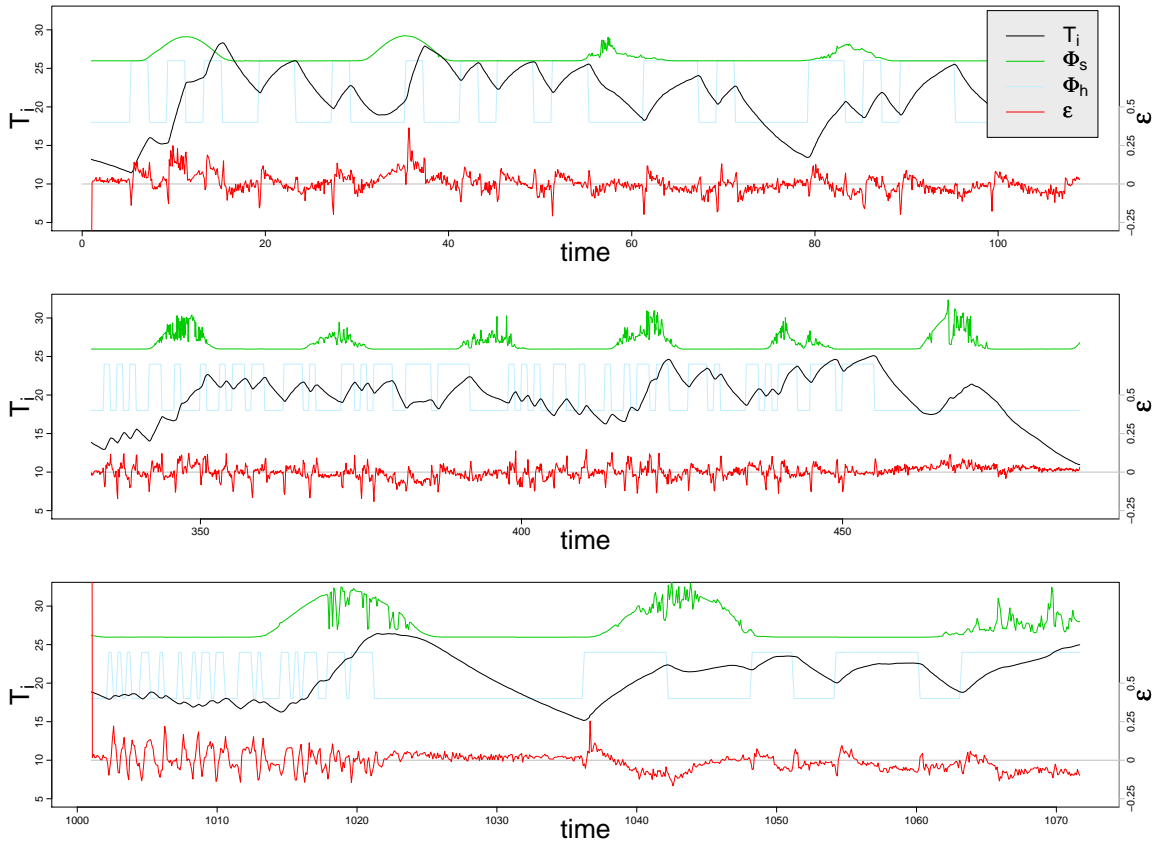
Plot of the error for Linear C is found in Figure 6.3(a). Comparison with the error from Linear B, reveals that the effect of high variance after state shifts of the heaters are still in the error and are similar, but non-stationarities have decreased. This is confirmed by the ACF and the periodogram in Figure 6.3(b). Both statistical functions show that the characteristics of the error are close to the characteristics of white noise.

6.5 Linear D

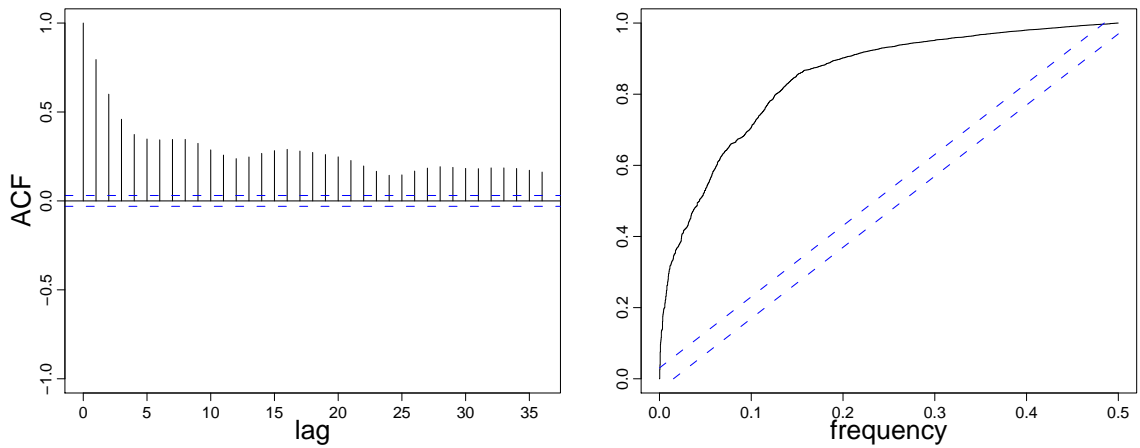
Plot of the error for Linear D is found in Figure 6.4(a). It is hard to visually find the difference in the error for Linear D compared to Linear C, but the ACF for Linear D in Figure 6.4(b) does reveal a correlation of lag 1 in the error, which is higher than for Linear C.

6.6 Linear E

Plot of the error for Linear E is found in Figure 6.5(a). As for Linear D it is difficult for find a visual difference from the error of Linear C. The ACF and the periodogram are very similar to those for Linear D.

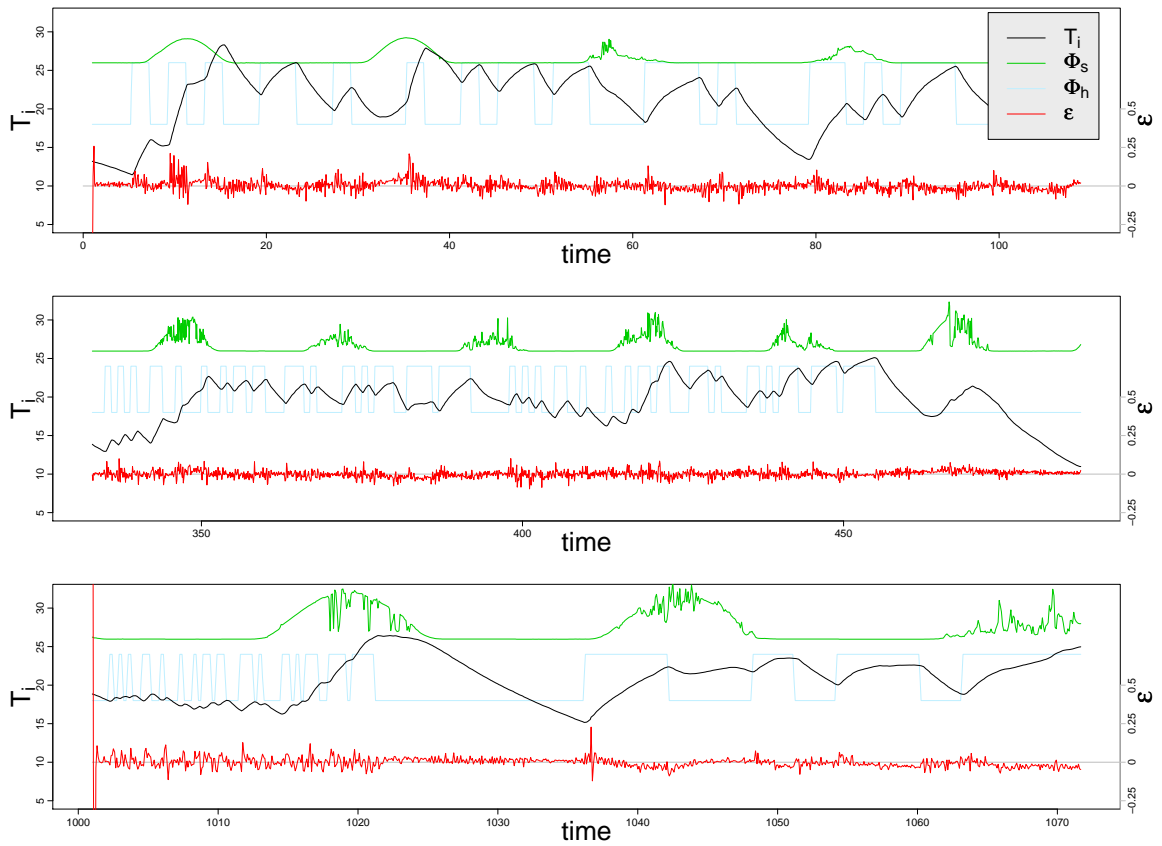


(a) Plot of the observed indoor temperature T_i , global irradiance Φ_s , heater signal Φ_h and one-step prediction error ϵ

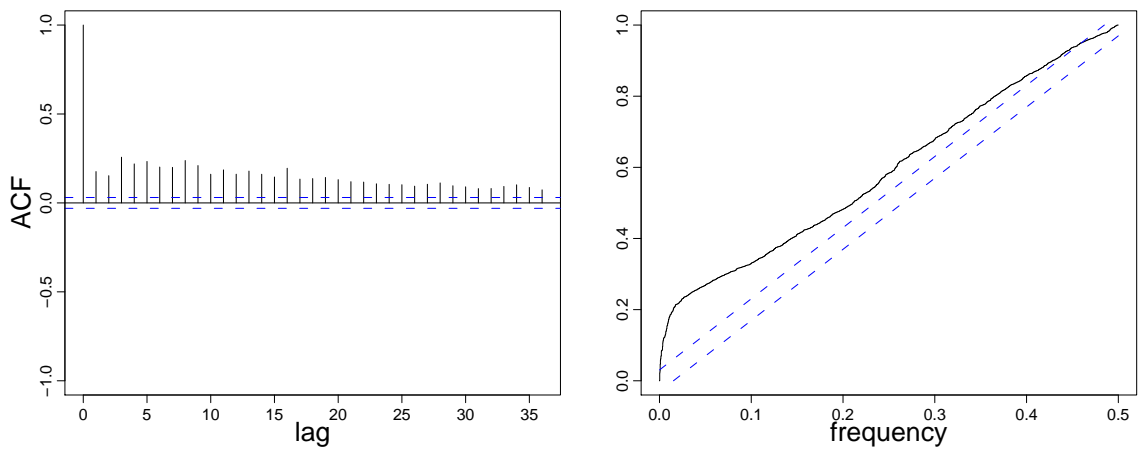


(b) Left plot is the ACF and right plot is the periodogram of the one-step prediction error ϵ .

Figure 6.1: Plots for Linear A.

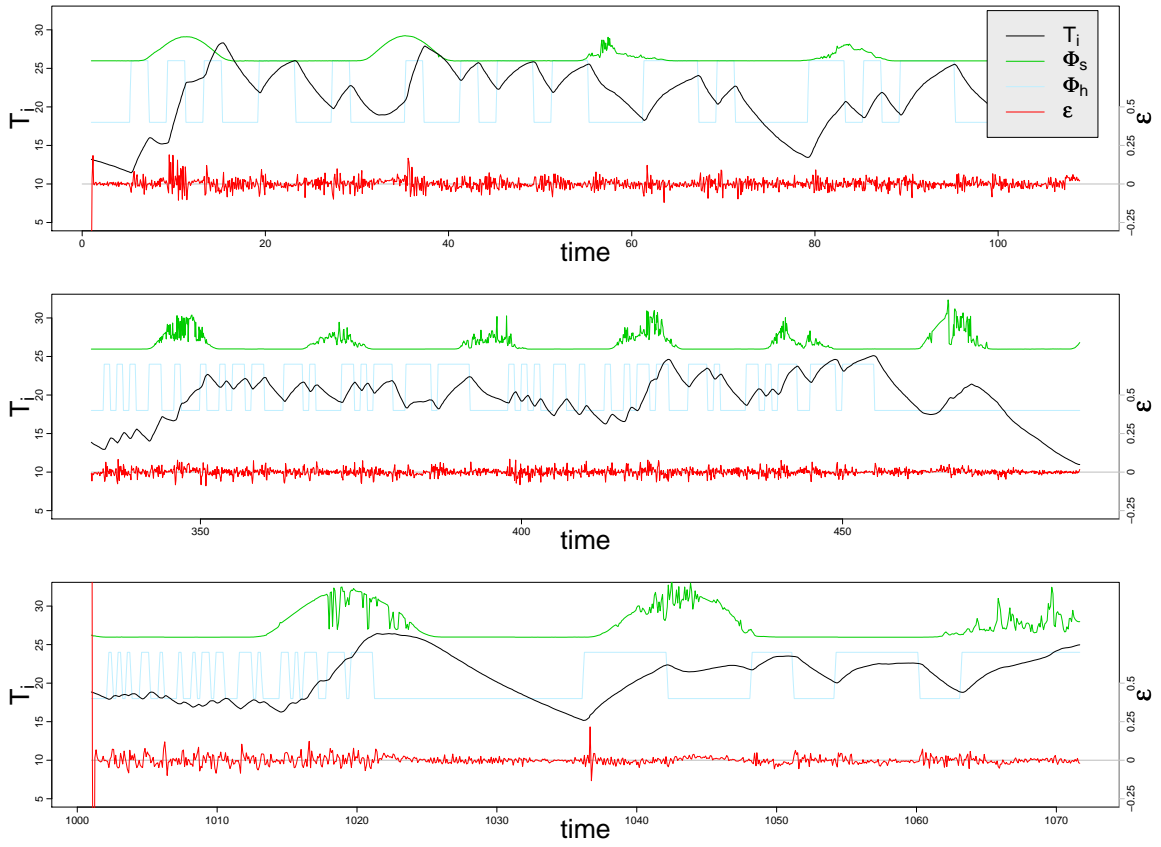


(a) Plot of the observed indoor temperature T_i , global irradiance Φ_s , heater signal Φ_h and one-step prediction error ϵ

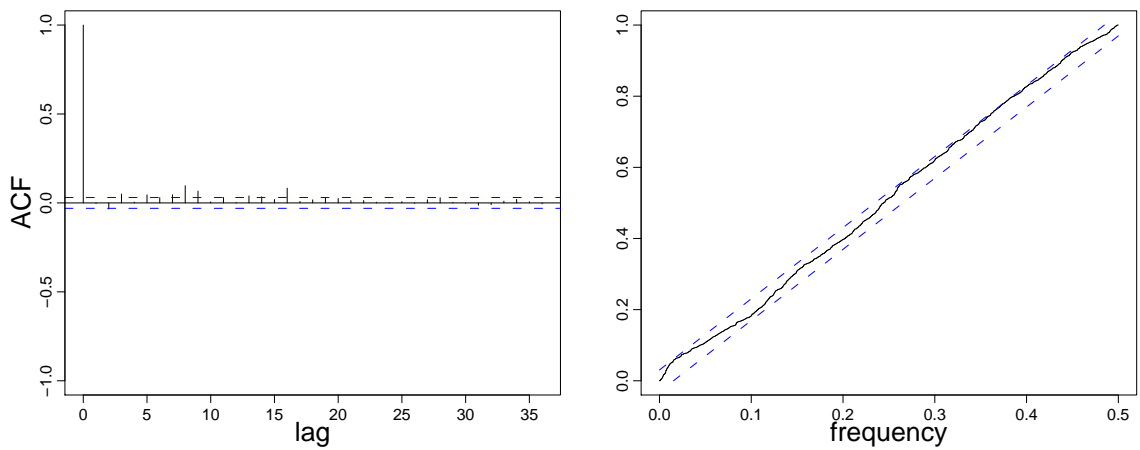


(b) Left plot is the ACF and right plot is the periodogram of the one-step prediction error ϵ .

Figure 6.2: Plots for Linear B.

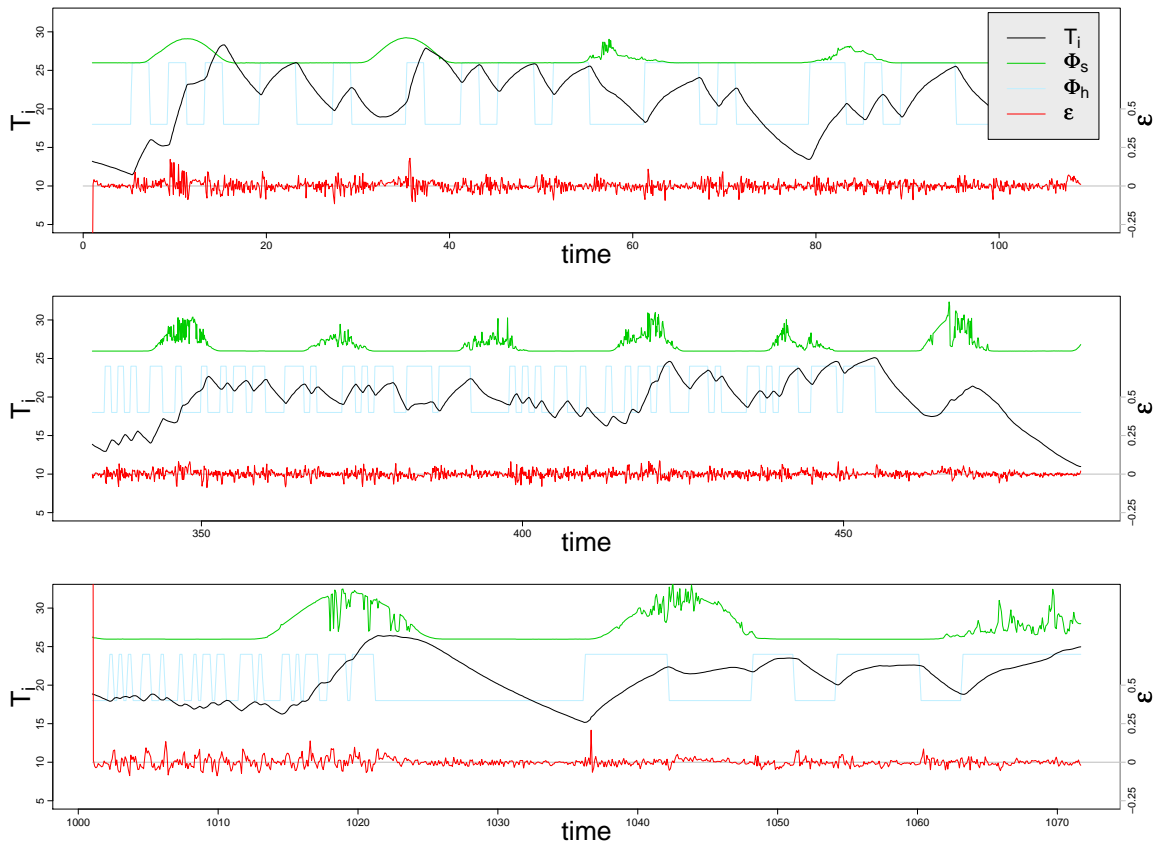


(a) Plot of the observed indoor temperature T_i , global irradiance Φ_s , heater signal Φ_h and one-step prediction error ϵ

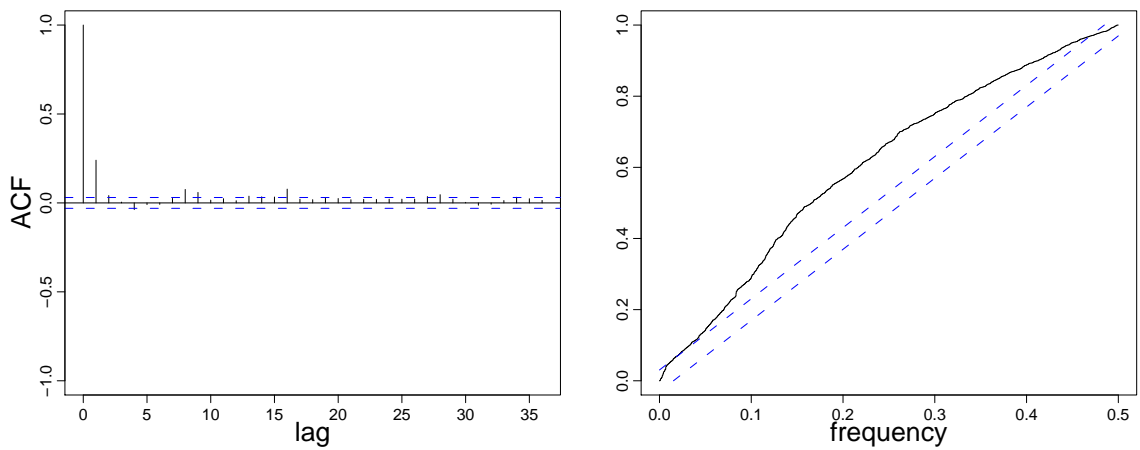


(b) Left plot is the ACF and right plot is the periodogram of the one-step prediction error ϵ .

Figure 6.3: Plots for Linear C.

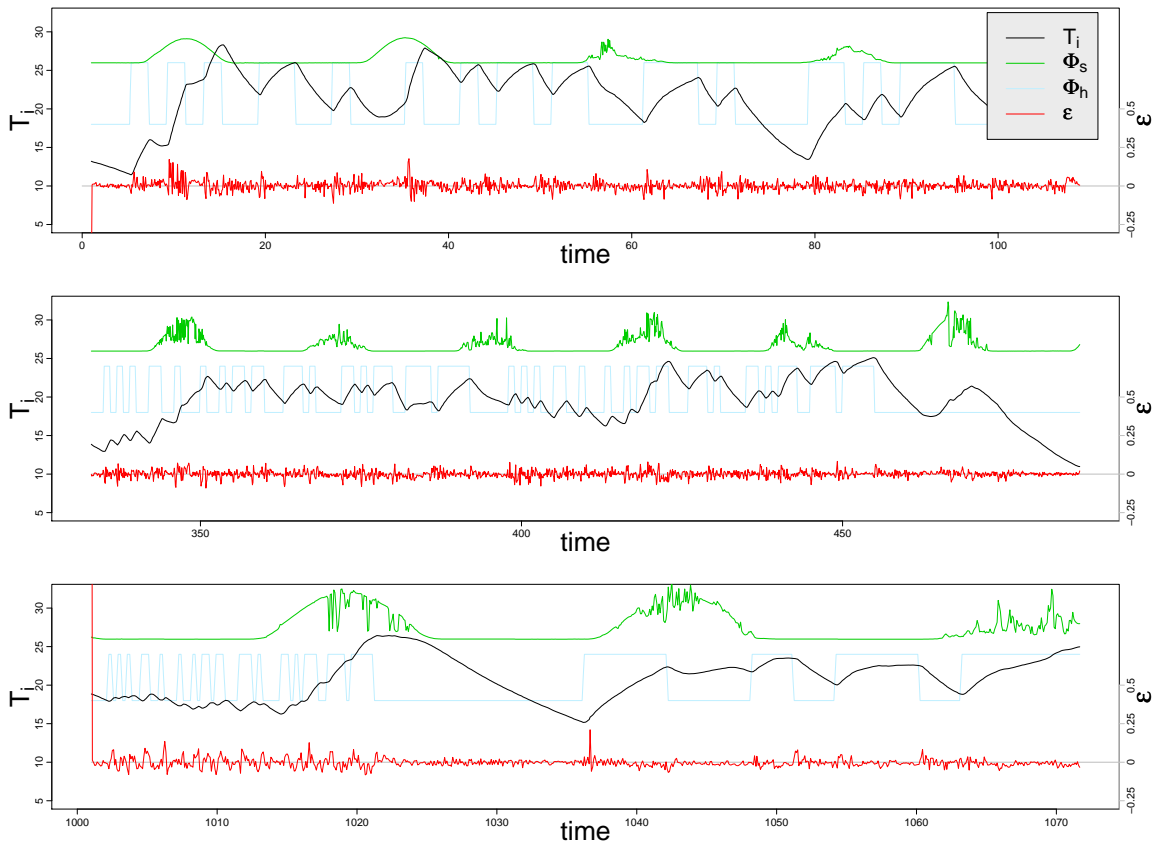


(a) Plot of the observed indoor temperature T_i , global irradiance Φ_s , heater signal Φ_h and one-step prediction error ϵ

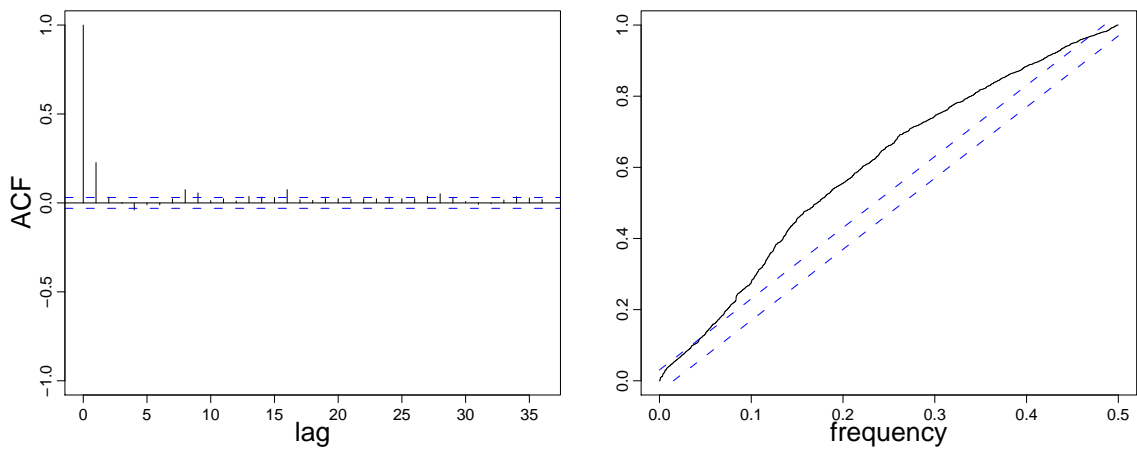


(b) Left plot is the ACF and right plot is the periodogram of the one-step prediction error ϵ .

Figure 6.4: Plots for Linear D.



(a) Plot of the observed indoor temperature T_i , global irradiance Φ_s , heater signal Φ_h and one-step prediction error ϵ



(b) Left plot is the ACF and right plot is the periodogram of the one-step prediction error ϵ .

Figure 6.5: Plots for Linear E.

Chapter 7

Results

This chapter presents the results from estimation of the selected models. First rough physical values of the physical parameters are calculated, and then the estimated values are evaluated.

7.1 Rough physical values

In order to evaluate the results of the estimated physical parameters in the models, knowledge of the real underlying values is needed. In this section physical considerations are used to calculate “rough” estimates of the values. Very little information of the building materials are at hand, and the calculated values here are therefore only used to give an idea of the magnitude of the values.

7.1.1 Heat capacities

The dimensions of the building used in the calculations are

$$L = 16.25\text{m} \quad (7.1)$$

$$W = 7.5\text{m} \quad (7.2)$$

$$H = 2.75\text{m}. \quad (7.3)$$

The specific heat capacities and densities of the building materials are from [3]. The heat capacity of the indoor air is calculated to be approximately

$$C_{\text{air}} = \rho_{\text{air}} \cdot c_{\text{air}} \cdot L \cdot W \cdot H \cdot \frac{1}{3600} = 0.11 \frac{\text{kWh}}{^{\circ}\text{C}} \quad (7.4)$$

where

$$c_{\text{air}} = 1.012 \frac{\text{J}}{\text{g}^{\circ}\text{C}} \quad \text{and} \quad \rho_{\text{air}} = 1.2041 \frac{\text{kg}}{\text{m}^3}. \quad (7.5)$$

The heat capacity of the plaster in the interior walls is calculated. Examining the FlexHouse layout (see Figure 1.1 at page 6) it is found that approximately 4 sides of interior wall is

along the long side of the building and 8 along the short side. Assuming a thickness of the plaster sheets of 10 mm gives

$$C_{\text{pl}} = (4L + 8W) \cdot H \cdot c_{\text{pl}} \cdot \rho_{\text{pl}} \cdot 0.01 \cdot \frac{1}{3600} = 1.16 \frac{\text{kWh}}{^{\circ}\text{C}}. \quad (7.6)$$

where

$$c_{\text{pl}} = 0.84 \frac{\text{J}}{\text{g}^{\circ}\text{C}} \quad \text{and} \quad \rho_{\text{pl}} = 1440 \frac{\text{kg}}{\text{m}^3}. \quad (7.7)$$

The heat capacity of the insulation material. It is assumed that rockwool sheets of 5 cm is inside the entire building envelope.

$$C_{\text{rw}} = 2(LW + LH + WH) \cdot c_{\text{rw}} \cdot \rho_{\text{rw}} \cdot 0.05 \cdot \frac{1}{3600} = 0.31 \frac{\text{kWh}}{^{\circ}\text{C}} \quad (7.8)$$

where

$$c_{\text{rw}} = 0.84 \frac{\text{J}}{\text{g}^{\circ}\text{C}} \quad \text{and} \quad \rho_{\text{rw}} = 70 \frac{\text{kg}}{\text{m}^3}. \quad (7.9)$$

Summing this gives a heat capacity of the building around

$$C_{\text{air}} + C_{\text{pl}} + C_{\text{rw}} = 1.57 \frac{\text{kWh}}{^{\circ}\text{C}} \quad (7.10)$$

This only covers a part of the building materials excluding wood, metal, and concrete etc. used in the walls and building envelope. Also the furnitures and computer hardware etc. will contribute to the heat capacity. Considering the heat capacity of the building estimated by Linear A to 3.42 kWh/°C, this leaves an unexplained heat capacity of approximately 2 kWh/°C. This is equivalent to a the heat capacity of concrete with a volume of

$$V_{\text{conc}} = \frac{2}{c_{\text{conc}} \cdot \rho_{\text{conc}} \cdot 3600} = 3.4 \text{m}^3 \quad (7.11)$$

where

$$c_{\text{conc}} = 0.88 \frac{\text{J}}{\text{g}^{\circ}\text{C}} \quad \text{and} \quad \rho_{\text{conc}} = 2400 \frac{\text{kg}}{\text{m}^3}. \quad (7.12)$$

Which is equivalent to a layer of 2.8 cm thick concrete evenly distributed over the base area of the building.

7.1.2 Window area

In an internal Risø report the window area of the south side of FlexHouse is measured to 10m². The same report measures that around 50% of the radiation energy passes through the windows. Since most of the solar irradiance will strike the southern side, a value of the effective window in the range of 5m² is reasonable.

7.2 Estimated physical parameters and time constants

The estimates of the physical parameters and the time constants of the selected models are found in Table 7.1. Note that the physical interpretation of each parameter is different for each model. Generally it can be said that the exact physical interpretation of the parameters and their values is difficult to give, and that the results should rather be interpreted relative to the models.

7.2.1 Heat capacities

The in Linear A estimated heat capacity of the building C_i is 3.42kWh/°C. This is found to be a reasonable value. For Linear B the added heat capacity C_h represent the heat capacity of the electrical heaters. The estimated value is close to the physically calculated value in (7.4). Since Linear B has just two time constants it is reasonable to believe that the large heat capacity to some extent represent the heat capacity of the building and the small the heat capacity of the indoor air.

Linear C has three heat capacities and it seems as if another part of the building is included in the model compared to Linear A and B. An exact physical interpretation of the heat capacities is difficult to give, and likewise for Linear D.

Name	Linear A	Linear B	Linear C	Linear D	Linear E
C_i	3.42	3.03	2.66	2.26	2.13
C_m	-	-	3.08	3.8	0.00102
C_e	-	-	-	0.018	4.82
C_h	-	0.0187	0.00384	0.00323	0.00361
R_{ia}	4.87	5.04	4.82	-	-
R_{ie}	-	-	-	4.9	0.963
R_{ea}	-	-	-	0.302	3.16
R_{ih}	-	10.2	33.3	63	62
R_{im}	-	-	3.45	1.68	4.76
A_w	10.7	8.05	5.53	4.54	3.77
A_e	-	-	-	-	21.8
τ_1	16.7	0.19	0.128	0.00513	0.00485
τ_2	-	15.3	3.97	0.203	0.224
τ_3	-	-	34.3	2.1	1.38
τ_4	-	-	-	35.8	22.7

Table 7.1: The estimated parameters. The heat capacities, C_x , are in [kWh/°C]. The heat flow resistances, R_x , are in [°C/kW]. The areas, A_x , are in [m²]. The time constants, τ_x , are in hours. Note that the physical interpretation of the parameters is different for each model.

The estimates for Linear E of two small and two large heat capacities, could be interpreted such that the two large represent the heat capacities of the solid materials in the building and the two small the heat capacity of the indoor air. This is not in compliance with the interpretation of the model formulation, so again it is found difficult to give an exact physical interpretation.

7.2.2 R-values and UA-values

The estimated value of R_{ia} for Linear A, B, and C, and for Linear D and E $R_{ie} + R_{ea}$, is used to find an estimate of the UA-value of the building by

$$\alpha_{UA} = \frac{1000}{R_{ia}} \frac{1}{L \cdot W} \quad (7.13)$$

or

$$\alpha_{UA} = \frac{1000}{R_{ie} + R_{ea}} \frac{1}{L \cdot W}. \quad (7.14)$$

This gives a UA-value in $W/(^{\circ}C \text{ m}^2)$. The estimated UA-values for the five considered models are found in Table 7.2 In [10] UA-values for single-family houses are estimated using regression models. The UA-values are U-values normalized with the ground area of the house. The results are UA-values in the range of 0.5 to 1 $W/(^{\circ}C \text{ m}^2)$ for single-family houses. The estimated values for FlexHouse, is according to this, quite high, indicating that the isolation of the building is poor. It is noted that a comparison of UA-values estimated by different modelling techniques and data basis, should not be carried out directly. The estimated values of parameters R_{ih} and R_{im} are not as important for the description of the insulation of the building.

7.2.3 Window area

The estimated effective window area A_w is found to be above the expected value around 5m^2 for Linear A, but for Linear C, D, and E, the value seems quite reasonable. The inclusion of an area A_e in Linear E, which represent how much solar energy is absorbed by the building envelope, seems to have only a small effect on A_w . The estimated value of A_e for Linear E is found reasonable.

7.2.4 Time constants

The single time constant for Linear A describes the slow dynamics. Linear B have two time constants, where the large time constant, which have approximately the same value

Name	Linear A	Linear B	Linear C	Linear D	Linear E
α_{UA}	3.63	3.50	3.66	3.39	4.28

Table 7.2: The UA-values of the building in $w/(^{\circ}C \text{ m}^2)$.

as for Linear A, describes the slow dynamics. The small time constant describes the fast dynamics, which is most likely related to the indoor air. A physical interpretation of the time constants for Linear C, D, and E are more complicated, and it is just concluded that the estimated values are found within a reasonable range.

Chapter 8

Further work

The following points should be taken into consideration and emphasized during further work.

8.1 Modelling with the present data

For further modelling with the present data the following should be considered

- Certainly the other models that can be combined from Linear E are interesting to evaluate.
- Including the wind speed and direction as inputs. This should be carried out by estimation of the impulse response function to find an appropriate way of entering them into the model. The state space model then becomes non-linear, and thus the maximum likelihood optimization will require considerably more computational power than for the linear models.
- A more in-depth analysis of the one-step prediction error, especially around the shifts in state of the electrical heaters. This is where the highest errors are observed. Plots of the error vs. the inputs should also be analysed.

8.2 Carrying out further experiments

When carrying further experiments the following should be considered

- A very informative step would be to conduct equivalent experiments in different buildings, and then compare the results of identical models.
- The sparse information of building materials has resulted in a poor comparison between the real underlying physical parameter values and the estimated values. Therefore it should be considered how such information about the building can be acquired.

- The temperature sensors must be cross validated to checked for bias before the experiments are carried out. The constant temperature difference between the rooms in the current data, see the discussion in Section 2.1, suggest that the sensors could be bias.
- Applying a different sampling strategy in the experiments can increase the embedded information in the signals. The implemented computer program in the building is currently logging all data at a constant samplerate, or at least trying to do so. The temperature sensors only send a value when the temperature has changed $\pm 0.5^{\circ}\text{C}$. Therefore the sampling strategy should be changed such that all the sent values are recorded with a time stamp. The data from the weather station should be recorded at a higher constant samplingrate. In the data pre-processing the signals can then be processed with higher order interpolation techniques, and then resampled with a constant samplerate. This should be carried out if possible.

Chapter 9

Conclusion

The aim of the study is to formulate and evaluate models of the heat dynamics of a building. This has been done on the basis of data from three experiments carried out in FlexHouse in February and March 2008. The evaluated models are grey-box models where a combination of prior physical knowledge and statistics is utilized. The input to the models consist of climate data measured at the location and measurements of the indoor temperature. It is found possible to estimate reasonable physical parameters for the heat dynamics of the building, including the time constants. Only linear models have been taken into consideration.

The estimates are maximum likelihood estimates and based on likelihood ratio tests a forward selection strategy has been used to find an optimal model. During the selection, five models of different complexity have been considered. The results from each of these models have been evaluated seperately. The simplest model have one time constant and the model selected as the optimal model has four time constants.

The results show that the absolute physical interpretation of the parameters in the models are difficult to give and that the interpretation is different for each model. The results for each model should thus be interpreted relative to the model, and the models can therefore be used to give information of changes in the isolation properties of a single building. Furthermore applying the same model on different buildings will make it possible compare characterization of heat dynamics for each building.

Appendix A

Input data to CTSM

Plots of the data used as input to CTSM. Each plot show the three input signals

- Φ_h the energy from the electrical heaters,
- T_a the ambient temperature,
- Φ_s the global irradiance,

and the observed indoor temperature T_i . Data from Experiment 3 is in Figure A.1, from Experiment 4 in Figure A.2, and from Experiment 6 in Figure A.3.

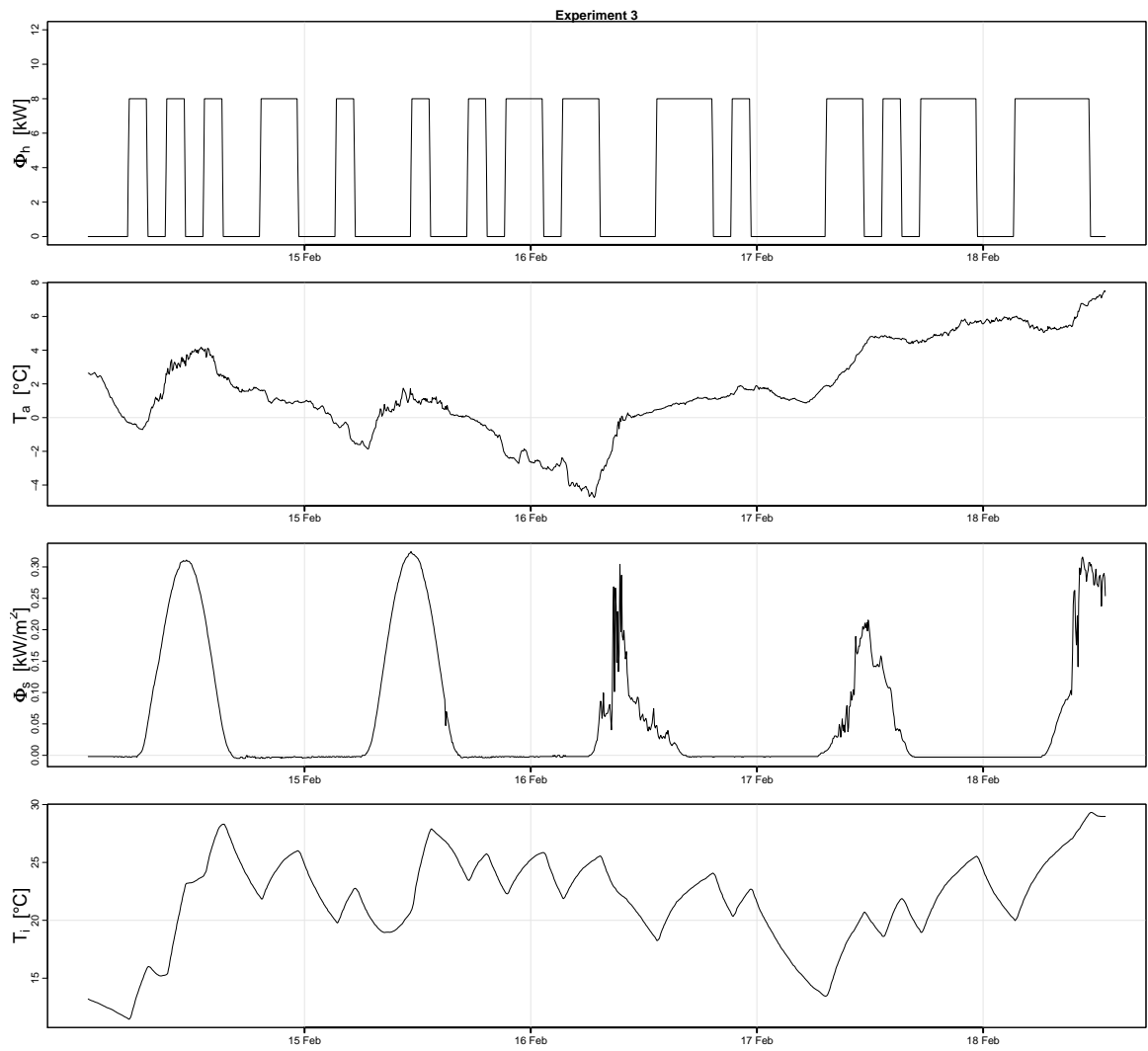


Figure A.1: The input to CTSM for Experiment 3.

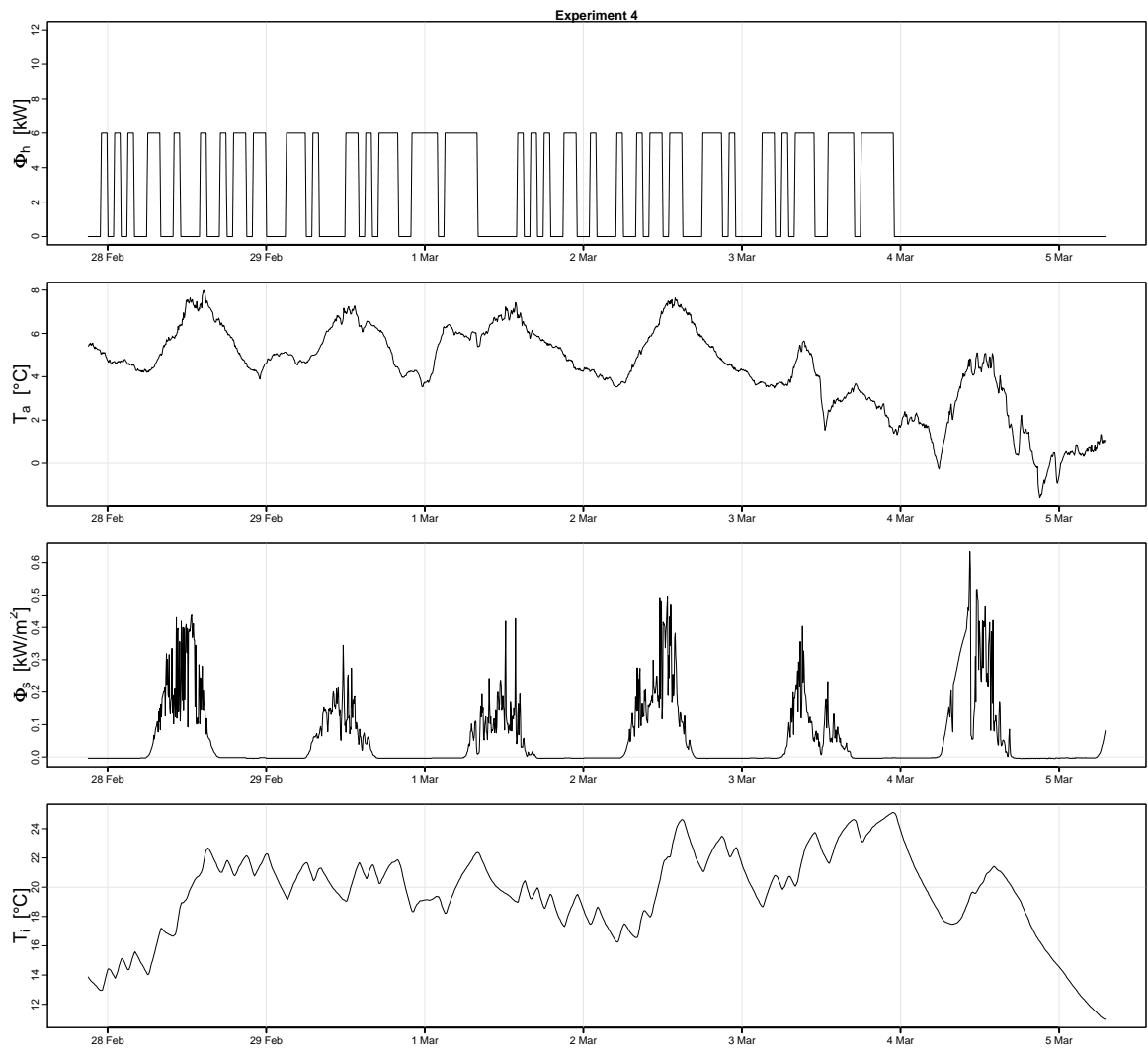


Figure A.2: The input to CTSM for Experiment 4.

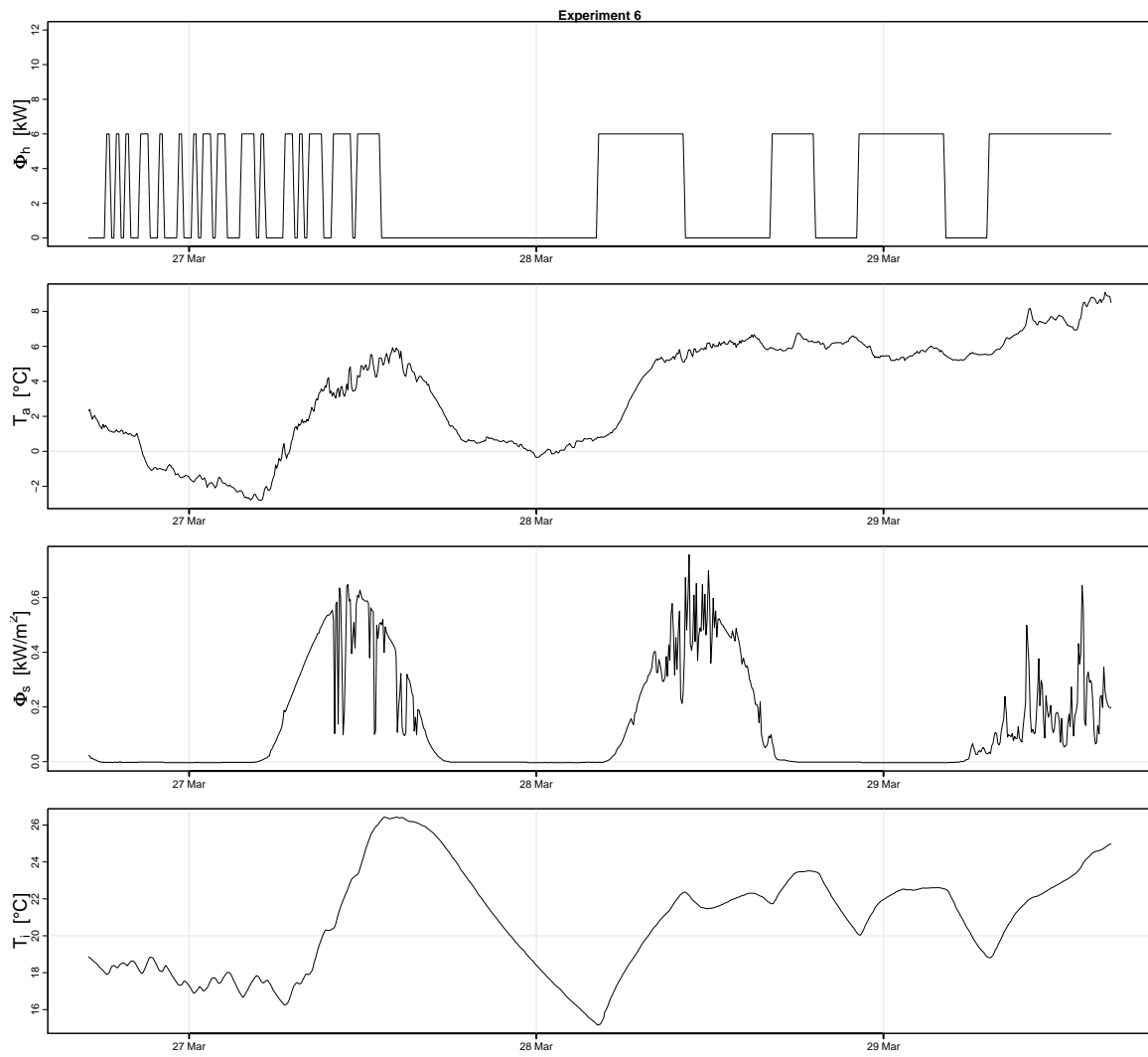


Figure A.3: The input to Ctsm for Experiment 6.

Bibliography

- [1] Klaus Kaae Andersen, Henrik Madsen, and Lars H. Hansen. Modelling the heat dynamics of a building using stochastic differential equations. *Energy and Buildings*, 31(1):13–24, 2000.
- [2] Ander Goikoetxea Arana. Flexhouse. Technical report, Risø DTU, 2007.
- [3] J.P. Holman. *Heat Transfer*. McGraw-Hill, ninth edition edition, 2002.
- [4] Tianzhen Hong, S.K. Chou, and T.Y. Bong. Building simulation: an overview of developments and information sources. *Building and Environment*, 35(4):347–361, 2000.
- [5] Niels Rode Kristensen and Henrik Madsen. Continuous time stochastic modelling, CTSM 2.3 - mathematics guide. Technical report, DTU, 2003.
- [6] Niels Rode Kristensen and Henrik Madsen. Continuous time stochastic modelling, CTSM 2.3 - user’s guide. Technical report, DTU, 2003.
- [7] H. Madsen and J. Holst. Estimation of continuous-time models for the heat dynamics of a building. *Energy and Buildings*, 22(1):67–79, 1995.
- [8] Henrik Madsen. *Time Series Analysis*. Chapman & Hall, 2007.
- [9] Henrik Madsen and J.M. Schultz. Short time determination of the heat dynamics of buildings. Technical report, DTU, 1993.
- [10] Henrik Aalborg Nielsen. Estimation of UA-values for single-family houses. Technical report, ENFOR, 2008.
- [11] Anders Thavlov, Peder Bacher, and Henrik Madsen. Data for energy performance analysis. Technical report, IMM, DTU, 2008.
- [12] Poul Thyregod and Henrik Madsen. *An introduction to general and generalized linear models*. IMM, DTU, 2006.